Journal of Visualized Experiments

Efficient and scalable generation of human ventral midbrain astrocytes from hiPSCs

--Manuscript Draft--

Article Type:	Invited Methods Collection - JoVE Produced Video
Manuscript Number:	JoVE62095R2
Full Title:	Efficient and scalable generation of human ventral midbrain astrocytes from hiPSCs
Corresponding Author:	Lucy A Crompton, PhD University of Bristol Bristol, Brsitol UNITED KINGDOM
Corresponding Author's Institution:	University of Bristol
Corresponding Author E-Mail:	NSLAC@bristol.ac.uk
Order of Authors:	Lucy A Crompton, PhD
	Sarah McComish
	Petros Stathakos
	Oscar Cordero-Llana
	Jon Lane
	Maeve A Caldwell
Additional Information:	
Question	**Response**
Please specify the section of the submitted manuscript.	Neuroscience
Please indicate whether this article will be Standard Access or Open Access.	Standard Access (US$2,400)
Please indicate the **city, state/province, and country** where this article will be **filmed**. Please do not use abbreviations.	Bristol, UK
Please confirm that you have read and agree to the terms and conditions of the author license agreement that applies below:	I agree to the UK Author License Agreement (for UK authors only)
Please provide any comments to the journal here.	I was told by the editor we will have a special lower cost to pay.

TITLE:

Efficient and Scalable Generation of Human Ventral Midbrain Astrocytes from Human-Induced Pluripotent Stem Cells

AUTHORS AND AFFILIATIONS:

Lucy A. Crompton[1*], Sarah F. McComish[2], Petros Stathakos[1], Oscar Cordero-Llana[3], Jon D. Lane[1#], Maeve A. Caldwell[2#]

[1]Cell Biology Laboratories, School of Biochemistry, University of Bristol, Bristol, UK
[2]Trinity College Institute of Neuroscience, Trinity College, Dublin, Ireland
[3]Regenerative Medicine Laboratory, School of Clinical Sciences, University of Bristol, Bristol, UK

#These authors contributed equally.

***CORRESPONDING AUTHOR**:
Lucy A. Crompton (Lucy.Crompton@bristol.ac.uk)

Email addresses of co-authors:
Sarah F. McComish (mccomiss@tcd.ie)
Petros Stathakos (petrosstathakos2017@gmail.com)
Oscar Cordero-Llana (oscar.corderollana@bristol.ac.uk)
Jon D. Lane (Jon.Lane@bristol.ac.uk)
Maeve A. Caldwell (Maeve.Caldwell@tcd.ie)

KEYWORDS:
astrocyte, Parkinson's disease, ventral midbrain, neuroinflammation, reactive human induced pluripotent stem cell, differentiation

SUMMARY:
Here, we present a method for reproducible generation of ventral midbrain patterned astrocytes from hiPSCs and protocols for their characterization to assess phenotype and function.

ABSTRACT:
In Parkinson's disease, progressive dysfunction and degeneration of dopamine neurons in the ventral midbrain cause life-changing symptoms. Neuronal degeneration has diverse causes in Parkinson's, including non-cell autonomous mechanisms mediated by astrocytes. Throughout the CNS, astrocytes are essential for neuronal survival and function, as they maintain metabolic homeostasis in the neural environment. Astrocytes interact with the immune cells of the CNS, microglia, to modulate neuroinflammation, which is observed from the earliest stages of Parkinson's, and has a direct impact on the progression of its pathology. In diseases with a chronic neuroinflammatory element, including Parkinson's, astrocytes acquire a neurotoxic phenotype, and thus enhance neurodegeneration. Consequently, astrocytes are a potential therapeutic target to slow or halt disease, but this will require a deeper understanding of their properties and roles in Parkinson's. Accurate models of human ventral midbrain astrocytes for in vitro study are

therefore urgently required.

We have developed a protocol to generate high purity cultures of ventral midbrain-specific astrocytes (vmAstros) from hiPSCs that can be used for Parkinson's research. vmAstros can be routinely produced from multiple hiPSC lines, and express specific astrocytic and ventral midbrain markers. This protocol is scalable, and thus suitable for high-throughput applications, including for drug screening. Crucially, the hiPSC derived-vmAstros demonstrate immunomodulatory characteristics typical of their in vivo counterparts, enabling mechanistic studies of neuroinflammatory signaling in Parkinson's.

INTRODUCTION:

Parkinson's disease affects 2%–3% of people over 65 years of age, making it the most prevalent neurodegenerative movement disorder[1]. It is caused by degeneration of ventral midbrain dopamine neurons within the substantia nigra, resulting in debilitating motor symptoms, as well as frequent cognitive and psychiatric issues[2]. Parkinson's pathology is typified by aggregates of the protein, α-synuclein, which are toxic to neurons and result in their dysfunction and death[1–3]. As the dopaminergic neurons are the degenerating population in Parkinson's, they were historically the focus of research. However, it is apparent that another cell type in the brain, the astrocytes, also demonstrate abnormalities in Parkinson's, and are believed to contribute to degeneration in models of Parkinson's[4–7].

Astrocytes are a heterogenous cell population that can transform both physically and functionally as required. They support neuronal function and health via a plethora of mechanisms, including the modulation of neuronal signaling, shaping of synaptic architecture, and trophic support of neuronal populations via secretion of specific factors[6,8–10]. However, astrocytes also have a substantial immunomodulatory role, integral to the development and propagation of neuroinflammation[10,11]. Neuroinflammation is observed in the affected brains, and significantly has recently been shown to pre-empt the onset of Parkinson's symptoms[12–15], thereby taking the center stage in Parkinson's research.

At a cellular level, astrocytes are said to become reactive in response to injury, infection, or disease, as an attempt to facilitate neuroprotection[9,6,10,16]. Reactivity describes a shift in astrocyte phenotype characterized by changes in gene expression, secretome, morphology, and mechanisms of clearance of cell debris and toxic byproducts[9–11,17]. This reactive shift occurs in response to inductive signals from microglia, which are the immune cells of the CNS and the first responders to injury and disease[9]. Both astrocytes and microglia respond to inflammatory signals by moderating their own function and can transduce inflammatory signals and thus directly influence neuroinflammation[9,10]. However, the chronic nature of Parkinson's results in a transition where reactive astrocytes become toxic to neurons, and themselves promote degeneration and disease pathology[6,9,10,18,19]. Significantly it was recently demonstrated that blocking the transformation of astrocytes into the reactive neurotoxic phenotype prevents the progression of Parkinson's in animal models[11]. Astrocyte reactivity in the paradigm of neuroinflammation has therefore become a major focus of Parkinson's research, and similarly relates to a wide spectrum of diseases of the CNS. Together these findings build a picture of

significant astrocytic involvement in the etiology of Parkinson's, emphasizing the need for accurate research models that recapitulate the phenotype of the human astrocyte populations that are involved in Parkinson's.

In the embryonic brain, neurons appear first, with the astroglial lineage, namely, the astrocytes and oligodendrocytes, appearing later in development[6]. In vivo and in vitro studies have highlighted a number of signaling pathways that appear to control the potency of neural progenitor cells from neuronal to astroglial derivatives. In particular, JAK/STAT, EGF, and BMP signaling play roles in the proliferation, differentiation, and maturation of astroglia[20,21]. These pathways have been the focus of in vitro protocols for the generation of astrocytes from pluripotent cells, including hiPSC[6,22,23]. There have been many successful examples of generating astrocytes from hiPSCs[6,24,25]. However, it is apparent that in vivo astrocytes in the CNS possess specific regional identities, which relate directly to their function, in accordance to the specific requirements of those astrocytes in relation to their specialized neuronal neighbors[17,24–26]. For example, relating specifically to the ventral midbrain, it has been demonstrated that astrocytes in this region express specific sets of proteins, including receptors for dopamine enabling communication with the local population of midbrain dopamine neurons[26]. Furthermore, ventral midbrain astrocytes demonstrate unique signaling properties[26]. Therefore, to study the role of ventral midbrain astrocytes in Parkinson's, we require an in vitro model that reflects their unique set of characteristics.

To address this, we have developed a protocol to generate ventral midbrain astrocytes (vmAstros) from hiPSCs. The resulting vmAstros exhibit characteristics of their in vivo ventral midbrain counterparts such as expression of specific proteins, as well as immunomodulatory functions. The results presented are from the differentiation of the NAS2 and AST23 hiPSC lines, which were derived and gifted to us by Dr. Tilo Kunath[27]. NAS2 was generated from a healthy control subject whereas AST23 is derived from a Parkinson's patient carrying a triplication in the locus encoding α-Synuclein (SNCA). These hiPSC lines have been previously characterized and used in a number of published research papers, including for the generation of various neural cell types[27–31].

PROTOCOL:

1. Human hiPSC line thawing, maintenance, and cryopreservation

1.1. Coating cell culture plates with vitronectin

1.1.1. For coating, dilute vitronectin to 5 µg/mL (1:100) in PBS at 1 mL per 10 cm^2 cell culture plate surface area. Leave for 1 h at room temperature.

1.1.2. Remove vitronectin and proceed immediately to adding hiPSCs/media to the culture plate.

NOTE**:** When removing vitronectin from the plate, it is crucial that the culture surface is not

allowed to dry out.

1.2. Thawing hiPSCs

1.2.1. Remove cryovials containing hiPSCs from liquid nitrogen and place in a 37 °C water bath until the contents have completely thawed.

1.2.2. Prepare 9 mL of prewarmed cell culture medium (e.g., E8 or E8 Flex) containing 1x cell supplement (e.g., Revitacell). Add 1 mL dropwise to the contents of the cryovial. Place the remaining 8 mL media into a 15 mL centrifuge tube and to this add the diluted contents of the cryovial.

CAUTION: Do not triturate the contents.

1.2.3. Centrifuge at 150 x *g* for 3 min. Aspirate the liquid without disturbing the cell pellet and resuspended in an appropriate volume of cell culture medium (e.g., E8 or E8 Flex) containing 1x cell supplement (e.g., Revitacell). For example, 2 mL per well of a 6-well plate.

1.2.4. Add resuspended hiPSCs to vitronectin coated dishes and place in 37 °C/5% CO_2 incubator.

NOTE: hiPSCs should start to attach to vitronectin coated plasticware in 30 min–2 h after thawing.

1.3. hiPSC maintenance

1.3.1. Maintain hiPSCs in cell culture medium (e.g., E8 or E8 Flex). Feed cells daily by media exchange. Always prewarm culture media for 30 min before feeding.

NOTE**:** If using E8 Flex, hiPSCs do not require media changes every 24 h and feeding increments can be extended to 48 h, if needed. Either E8 Flex or E8 media yield equally high-quality hiPSC cultures. HiPSCs should be cultured for a minimum 14 days post-thawing, and prior to beginning the differentiation steps. Culture periods of less than 14 days appear to negatively impact the survival of the hiPSCs during the initial differentiation period.

1.4. Passaging hiPSCs

NOTE: Passage hiPSCs at approximately 80% confluency (**Figure 1A**: 3–4 day passaging interval).

1.4.1. 1 h prior to beginning, add 1x cell supplement (e.g., Revitacell) to the hiPSC culture.

1.4.2. Wash hiPSCs once with PBS (without calcium or magnesium) and add 0.5 mM EDTA (diluted from stock in PBS without calcium or magnesium).

1.4.3. Incubate for 5 min at room temperature, or until the hiPSCs begin to detach from each other and take on a more rounded appearance, with the boundaries of each iPSC appearing brighter under a brightfield microscope.

1.4.4. Add 200 µL EDTA on to a focused area of the hiPSCs with a pipette. If they readily detach, making a clear space in the cell layer, then they are ready to be harvested. If they do not readily detach, leave in EDTA and repeat after 1 min.

1.4.5. When ready to proceed, gently remove EDTA, and using a pipette, gently wash the hiPSCs twice with cell culture medium (e.g., E8 or E8 Flex).

NOTE: To achieve this without the hiPSCs detaching, tip the plate and add media dropwise down the side of the culture plate.

1.4.6. To harvest hiPSCs use 1 mL cell culture medium (e.g., E8 or E8 Flex) containing 1x cell supplement (e.g., Revitacell). Release the media directly onto the hiPSC layer and the cells should detach. If required, repeat with another 1 mL media.

1.4.7. View the hiPSCs under the microscope. Ideally, hiPSCs should appear in relatively uniform clusters as shown in **Figure 1B**. If hiPSC clusters are much larger, or very variable in size, use the pipette to break up the larger hiPSC clusters (**Figure 1B**).

NOTE**:** Do not over-triturate hiPSCs. Although the supplement increases the overall cell survival, over trituration negatively impacts on the survival of the hiPSC culture. 1–4 passes with a pipette are recommended.

1.4.8. Using a serological pipette, transfer the hiPSC suspension on to a vitronectin-coated plate as prepared in **section 1.1**. Return the hiPSC culture to the 37 °C/5% CO_2 incubator.

1.5. hiPSC line cryopreservation

NOTE: Cryopreserve hiPSCs at approximately 80% confluency.

1.5.1. 1 h prior to beginning, add 1x cell supplement (e.g., Revitacell) to the hiPSC culture.

1.5.2. Detach hiPSCs from culture plates using 0.5 mM EDTA as described in **section 1.4**, collecting cells in cell culture medium (e.g., E8 or E8 Flex) containing 1x cell supplement (e.g., Revitacell). Centrifuge at 150 x *g* for 3 min.

1.5.3. Resuspend pelleted hiPSCs in cell freezing media (see **Table of Materials**). Use 700 µL per 10 cm^2 culture area, equivalent to 1 cryovial of cells per well of a 6-well plate.

1.5.4. Transfer cryovials into an appropriate cell freezing vessel (for details see **Table of Materials**).

1.5.5. Transfer the freezing vessel to a -80 °C freezer for 24 h. After 24 h, cryovials can be transferred to liquid nitrogen (-196 °C) for long-term storage.

2. vmAstro Differentiation protocol

NOTE: A schematic summary of the vmAstros differentiation protocol is shown in **Figure 1A**. A detailed list of reagents required for the protocol and their preparation is given in **Table 1**.

2.1. Differentiation and expansion of vmNPCs

NOTE: This protocol has been optimized to begin with a minimum with 1x well of a 6-well plate (10 cm^2) of hiPSCs 70%–80% confluency, which is approximately 4–5 x 10^4 cells/cm^2 (**Figure 1B**)[30]. Starting cell number and density must be optimized for each hiPSC line as it significantly impacts survival and differentiation efficiency.

2.1.1. Remove cell culture medium from hiPSCs and wash 3x in DMEM/F12 + glutamax. Replace media with 2 mL vmNPC induction media (N2B27 + CHIR99021 + SB431542 + SHH(C24ii) + LDN193189. See **Table 1** for details of preparing media and reagents).

2.1.2. Feed on alternate days with a half media change after 24 h, and a full media change at 48 h.

NOTE: After 3–4 days the vmNPC culture will require passaging. A standard passaging ratio of 1:3 or 1:4 is recommended—this needs to be optimized for each hiPSC line used.

2.1.3. 1 h before passaging, add 1x cell supplement (e.g., Revitacell) to vmNPCs, and prepare 1x basement membrane matrix (e.g., Geltrex) coated tissue culture plastic (**section 2.2**).

2.1.4. Remove the media from vmNPCs and wash 2x with D-PBS. Add 1 mL pre-warmed cell detachment solution (e.g., Accutase) per 10 cm^2 culture area (1 mL per well of a 6-well plate).

2.1.5. Place at 37 °C for 1 min and then examine vmNPCs using a phase contrast microscope.

NOTE: The vmNPCs will start to round up, their processes will re-tract, and gaps will appear in the cell layer. This can take from 1–3 min depending on cell density.

2.1.6. When vmNPCs take on this appearance, add 100 µL of cell detachment solution (e.g., Accutase) on to the layer of vmNPCs.

NOTE: If the vmNPCs are ready to detach, a hole in the cell layer will appear. If this doesn't happen, then the vmNPCs require further incubation with cell detachment solution.

2.1.7. If vmNPCs readily detach, then gently remove the cell detachment solution and wash vmNPCs 2x with N2B27. Add the N2B27 down the side of the well or culture vessel and gently swirl to wash, ensuring that vmNPCs do not detach.

NOTE: This step must be completed quickly to ensure vmNPCs do not reattach to the cell surface. If vmNPCs start to detach in the wash steps, collect via centrifugation at 150 x *g* for 3 min. vmNPCs are not centrifuged as standard when passaging as this can reduce their survival.

2.1.8. Finally, remove vmNPCs using a pipette, by vigorously ejecting vmNPC induction media containing 1x cell supplement (e.g., Revitacell) directly on to the cell layer. This should remove vmNPCs, which can then be transferred to a 15 mL centrifuge tube.

NOTE: Do not use the resuspended vmNPCs to remove further cells as this will result in their over-trituration, which reduces their survival.

2.1.9. Replace in 37 °C/5% CO_2 incubator. vmNPCs should begin to attach to the matrix-coated surface after 20–30 min. Replace half of the media with fresh vmNPC induction media (without cell supplement) after 24 h and continue the feeding schedule as earlier.

2.1.10. Continue the regime of feeding and passaging for 10 days.

2.2. Preparing basement membrane matrix and coating tissue culture plastic

NOTE: For maintaining vmNPCs 1x basement membrane matrix (e.g., Geltrex) is used for coating plasticware. For maintaining vmAPCs or vmAstros, 0.25x basement membrane matrix can be used.

2.2.1. Remove basement membrane matrix stock from a -80 °C freezer and place in a 4 °C fridge overnight to thaw.

2.2.2. Dilute 1:10 with ice cold DMEM/F12 + glutamax, aliquot and store at -80 °C as a 10x stock.

2.2.3. When coating plasticware dilute this 10x stock to 1x (for vmNPCs) or 0.25x (for vmAPCs or vmAstros) with ice cold DMEM/F12 + glutamax.

2.2.4. Immediately add to tissue culture plastic at 1 mL per 10 cm^2, for example, 1 mL per well of a 6-well plate.

2.2.5. Place at 37 °C for 1 h. The basement membrane matrix solution should not be removed from plasticware until ready to add media/cells to ensure the coated plasticware does not dry out. Matrix coated plates do not require washing before adding cells.

2.3. Expansion of vmNPCs

2.3.1. On day 10 of the protocol, replace the induction media with vmNPC expansion media (N2B27 + GDNF + BDNF + ascorbic acid. See **Table 1** for details of preparing media and reagents).

NOTE**:** The vmNPCs do not require the addition of mitogens to induce proliferation. BDNF, GDNF, and ascorbic acid support the survival and maintenance of vmNPCs[30].

2.3.2. Feed on alternate days with a half media change after 24 h, and a full media change at 48 h.

NOTE: After 3–4 days, the vmNPC culture will require passaging. For passaging, a standard passaging ratio of 1:3 or 1:4 is recommended (this needs to be optimized for each hiPSC line used. Determine the ratio that gives the best survival, proliferation, and generation of vmNPCs).

2.3.3. 1 h before passaging, add 1x cell supplement (e.g., Revitacell) to vmNPCs, and prepare 1x matrix coated plates/flasks in advance (**section 2.2**). Prewarm the cell detachment solution (e.g., Accutase) to 37 °C. Prewarm fresh vmNPC expansion media containing 1x cell supplement (e.g., Revitacell).

2.3.4. Remove media from vmNPCs and wash 2x with D-PBS. Add 1 mL cell detachment solution (e.g., Accutase) per 10 cm^2 culture area (1 mL per well of a 6-well plate). Place at 37 °C for 1 min and then examine vmNPCs using a phase-contrast microscope.

NOTE: The vmNPCs will start to round up, their processes will re-tract, and gaps will appear in the cell layer. This can take from 1–3 min depending on the cell density.

2.3.5. When vmNPCs takes on a rounded appearance, add 100 µL of cell detachment solution (e.g., Accutase) on to the layer of vmNPCs.

NOTE: If the vmNPCs are ready to detach, a hole in the cell layer will appear. If this doesn't happen, then the vmNPCs require further incubation with the cell detachment solution.

2.3.6. If vmNPCs do readily detach, then gently remove the cell detachment solution and wash vmNPCs twice with N2B27. Add the N2B27 down the side of the well or culture vessel and gently swirl to wash, ensuring that vmNPCs do not detach.

NOTE: If vmNPCs start to detach in the wash steps, collect via centrifugation at 150 x *g* for 3 min. vmNPCs are not centrifuged as standard when passaging as this can reduce their survival. This step must be completed quickly to ensure vmNPCs do not reattach to the cell surface.

2.3.7. Remove vmNPCs using a pipette, and vigorously eject vmNPC expansion media containing 1x cell supplement (e.g., Revitacell) directly on to the cell layer. This should remove vmNPCs, which can then be transferred to a 15 mL centrifuge tube.

NOTE: Do not use the resuspended vmNPCs to remove further cells as this will result in their over-trituration, which reduces their survival.

2.3.8. Replace in 37 °C/5% CO_2 incubator. vmNPCs should begin to attach to the matrix coated surface after 20–30 min. After 24 h, replace half of the culture media with fresh vmNPC expansion media (without cell supplement) and continue the previous feeding schedule.

2.3.9. Continue this regime of feeding and passaging for 10 days. vmNPCs can be expanded up to day 50.

2.4. Differentiation and expansion of vmAPCs

NOTE: vmNPCs cultures expanded as in section 3.2 can be used successfully for the generation of vmAPCs/vmAstros anywhere between 30 and 50 days from the initial hiPSC stage (**Figure 1A**).

2.4.1. Take a confluent vmNPC culture and wash vmNPCs 3x in advanced DMEM/F12 to remove traces of the components of vmNPC expansion media. Replace the media with vmAPC expansion media (ASTRO media +EGF +LIF. See **Table 1** for details of preparing media and reagents).

2.4.2. After 72 h passage, the vmNPC culture is at a high ratio (1:7.5). Passage using cell detachment solution as described for vmNPC in **section 2.3.** For example, assuming vmNPCs were maintained in a single well of a 6-well plate, they should now be passaged into a 1x matrix coated 75 cm^2 flask (coated as described in **section 2.2**).

2.4.3. Resuspend vmNPCs in an appropriate volume of vmAPC Expansion media (7.5–15 mL media per 75 cm^2 flask. Complete media changes every 3 days, or as the cells require.

NOTE: From this point on, vmNPCs are referred to as vmAPCs and should be passaged as single cells rather than cell clusters. vmAPCs should be passaged every 3–7 days or as they become confluent to avoid becoming over confluent. From this point onward the reduced concentration of 0.25x matrix should be used to coat plasticware (as described in **section 2.2**).

2.4.4. Expand vmAPCs until they reach day 90 (from the hiPSC stage), cryopreserving vmAPCs at various points in their expansion.

2.5. Generation of mature vmAstros from vmAPCs

NOTE: At this stage, vmAPCs can be grown in 175 cm^2 tissue culture flasks. This may be expanded for the generation of large numbers of mature vmAstros.

2.5.1. When vmAPCs reach 80% confluency, wash 3x with ASTRO media and replace with vmAstros maturation media (ASTRO media +BMP4 +LIF. See **Table 1** for details of preparing media and reagents).

2.5.2. Carry out a complete media change every 3 days, or as the cells require, for 10 days.

NOTE: a) At this point, characterization indicates that the vmAstros are mature, as confirmed by immunocytochemistry (**Figure 2G–I**) and by gene expression analysis (manuscript in preparation). b) vmAstros used immediately after maturation should be re-plated on a newly prepared matrix-coated surface. Maintaining either vmAPCs or vmAstros on the same culture surface for over 14 days could lead to suboptimal cultures, where cells begin to shrink in size and even detach. c) For applications examining neuroinflammatory modulation, BMP4 and LIF should be removed from the vmAstros 72 h prior to cytokine treatment as these factors can interfere with the efficacy of the cytokine treatment (data not shown).

2.5.3. vmAstros can now be re-plated for experimental assays, for example, onto coverslips for immunocytochemistry or cryopreserved for future applications (**sections 3, 4**).

NOTE: Passaging should not be necessary at this stage of the protocol as proliferation should only occur at a very low rate. vmAPCs plated too densely at this stage maintain higher levels of proliferation. If this is the case, passage and split cells to achieve a density as is shown in **Figure 1F**.

3. Cryopreservation of vmNPCs, vmAPCs, and vmAstros

NOTE: Cryopreserve vmNPCs/vmAPCs/vmAstros at full confluency.

3.1. 1 h prior to beginning, add 1x cell supplement (e.g., Revitacell) to culture. Fill the cryostorage vessel (see **Table of Materials**) with isopropanol at room temperature.

3.2. Detach the cells from the culture plates using cell detachment solution as described in **sections 2.3, 2.4, and 2.5**, collecting cells in appropriate media (N2B27 or ASTRO media) containing 1x cell supplement (e.g., Revitacell). Centrifuge at 150 x *g* for 3 min.

3.3. Resuspend pelleted vmNPCs/vmAPCs/vmAstros in cell freezing media (see **Table of Materials**) volumes as follows (**steps 3.3.1. – 3.3.3.**)

3.3.1. For vmNPCs: 700 µL per 10 cm^2 culture area, into 1 cryovial.

3.3.2. For vmAPCs: 700 µL per 60 cm^2 culture area, into 1 cryovial (approximately 1/3 of a T175 culture flask).

3.3.3. For vmAstros: Resuspend in a 2 mL of media and count the number of vmAstros. Re-centrifuge and resuspend in cell freezing media (see **Table of Materials**) at a number per cryovial appropriate to future applications. Assuming an approximate cell loss of 15% due to freeze-thawing, newly thawed vmAstros are counted and plated with a 15% excess cell number to

compensate for cell death in the freeze-thaw process. This is, therefore, equivalent to 74,750 vmAstros per cm^2. Thawed vmAstros are maintained for 72 h in ASTRO media prior to assaying.

3.4. Transfer the cryovials into a cell freezing vessel (for details see **Table of Materials**) and transfer the freezing vessel to a -80 °C freezer for 24 h. After 24 h, cryovials can be transferred to liquid nitrogen (-196 °C) for long-term storage.

4. Characterization of vmAstro phenotype by immunocytochemistry

4.1. Coverslip preparation and plating of vmAstros

4.1.1. Place 100–200 13 mm glass coverslips in glass Petri dishes on a layer of filter paper and sterilize them in a dry autoclave.

4.1.2. Transfer the coverslips to wells of 4- or 24-well plates using sterile forceps. Add 1x matrix solution (e.g., Geltrex) on the coverslips as 50 μL droplets and incubate at 37 °C for 1 h.

4.1.3. Passage or thaw vmAstros, resuspend in ASTRO media and carry out a count. Plate vmAstros at 25–100,000 cells per coverslip in a 50 μL droplet.

4.1.4. Remove the matrix from the coverslip and immediately add vmAstros in a droplet of media. Place at 37 °C for 30 min and then flood the wells with an additional 250 μL ASTRO media.

4.2. Fixation

NOTE: If carrying out immunocytochemistry to simply check for astrocyte and midbrain marker expression, vmAstros can be fixed 24 h after plating.

4.2.1. Prepare 4% formaldehyde solution by diluting 36% formaldehyde solution 1:9 in D-PBS.

4.2.2. Wash vmAstros 1x with D-PBS. Immediately add 4% formaldehyde to the wells and leave at room temperature for 10 min.

4.2.3. Remove formaldehyde and replace with D-PBS. Either store at 4 °C or proceed to immunocytochemistry.

4.3. Immunocytochemistry

4.3.1. Wash coverslips in wells 3x with D-PBS. Permeabilize and block in 10% goat serum, 1% BSA in 0.1% PBTx (D-PBS + 1:1000 Triton-X) for 1 h at room temperature.

4.3.2. Add primary antibodies (**Table of Materials**) in 1% goat serum, 0.1% BSA in 0.1% PBTx (D-PBS + 1:1000 Triton-X) and incubate overnight at 4 °C on a rocker.

4.3.3. On the next day, remove primary antibodies and wash coverslips 3x with D-PBS.

4.3.4. Add appropriate secondary antibodies (**Table of Materials**) in 1% goat serum, 0.1% BSA in 0.1% PBTx, and incubate for 1–2 h at room temperature and protect it from light on a rocker. Wash coverslips 3x with D-PBS.

4.3.5. Add DAPI solution (0.1 μg/mL DAPI in D-PBS) and incubate at room temperature for 10 min. Wash coverslips 3x with D-PBS.

4.3.6. To mount the coverslip, add a 5 μL droplet of Mowiol/DABCO mounting media [12% Mowiol (w/v), 12% glycerol (w/v) dissolved overnight stirring in 0.2 M Tris (pH 8.5) with 25 mg/mL 1,4-diazabicylo[2.2.2]octane (DABCO)] to a glass microscope slide. Using forceps, carefully remove the coverslip from the well; dab the edge of the coverslip on the tissue to remove the excess liquid and place vmAstros side down onto the Mowiol/DABCO droplet.

4.3.7. Repeat for each coverslip and leave to dry for 8 h before microscopic examination.

4.4. Measurement of vmAstros secretion of IL-6 in response to cytokine treatment

4.4.1. Cytokine treatment of vmAstros and media collection

NOTE: Following the 10-day maturation with BMP4 and LIF, vmAstros should be passaged, counted, and plated on 0.25x matrix-coated tissue culture plasticware (as detailed in **section 2.2**), at a density of 65,000 vmAstros per cm^2 in ASTRO media. BMP4 and LIF should be removed from the vmAstros 72 h prior to cytokine treatment as active signaling from these factors can interfere with the efficacy of the cytokine treatment. Alternatively, cryopreserved vmAstros can be thawed and used for assays.

4.4.1.1. On the day of the assay, gently wash vmAstros 3x in non-redox media (DMEM/F-12 + glutamax + N2).

4.4.1.2. Use an untreated control and cytokine-treated well for comparison. Add chosen cytokine at optimized concentration. The data in **Figure 2J–L** were generated using IL-1α at 3 ng/mL[9] in non-redox media at 1 mL per 10 cm^2 cell culture area.

4.4.1.3. Replace vmAstros in 37 °C/5% CO_2 incubator for 24 h. After 24 h, collect culture media into sterile microfuge tubes.

4.4.1.4. If ELISA will not be carried out immediately, snap freeze media samples by submerging microfuge tubes in liquid nitrogen and store at -80 °C for future analysis.

4.4.2. ELISA measurement of IL-6 concentration in culture media

NOTE: The following protocol is optimized specifically for use with the IL-6 ELISA kit detailed in

the **Table of Materials**. Antibodies and standards delivered as lyophilized powder in a new ELISA kit must be reconstituted prior to first use, and aliquoted for future use. The data sheet provided with the kit details the reagents and volumes required for reconstitution. The capture antibody must be reconstituted in PBS (without carrier protein).

4.4.2.1. Perform the ELISA in a 96-well plate format and calculate the volumes of reagents according to the wells used. On the day of ELISA, prepare capture antibody by diluting stock 1:120 in PBS. Coat the plate by loading 50 µL of capture antibody per well. Cover the plate with an adhesive strip and incubate at room temperature overnight.

4.4.2.2. Next day, wash the plate 3x with D-PBS-Tween (D-PBS with 0.05% Tween-20), 400 µL per well. Blot dry.

4.4.2.3. Block the plate by loading 150 µL D-PBS/1% BSA per well. Incubate at room temperature for at least 1 h followed by a wash (as **step 4.4.2.2.**).

4.4.2.4. Thaw samples on ice (this can take 1–2 h). Dilute samples 1:5 by loading 10 µL sample and 40 µL D-PBS/1% BSA. Vortex every sample prior to loading.

NOTE: It is necessary to dilute samples when carrying out an IL-6 ELISA, dilutions should be optimized.

4.4.2.5. Prepare the top standard (1,000 ρg/mL) by diluting stock 1:180 in D-PBS/1% BSA. Prepare 7 standards by carrying out a serial dilution of the top standard. Vortex between each dilution.

4.4.2.6. Add 50 µL of standards/samples to wells. Use D-PBS/1% BSA as the blank. Incubate at room temperature for 2 h on an orbital shaker to properly mix the diluted samples.

4.4.2.7. Wash the plate as in **step 4.4.2.2.**

4.4.2.8. Prepare detection antibody by diluting stock 1:60 in D-PBS/1% BSA. Load 50 µL of detection antibody per well. Cover the plate and incubate at RT for 2 h, followed by a wash (as in **step 4.1.1.2.**).

4.4.2.9. Prepare streptavidin conjugated to horseradish peroxidase (Strep-HRP) by diluting stock 1:40 in D-PBS/1% BSA. Load 50 µL Strep-HRP per well and incubate at room temperature for 20 min in the dark, followed by a wash (as in **step 4.4.2.2.**).

4.4.2.10. Initiate the color reaction by loading 50 µL TMB substrate solution per well. Incubate at room temperature in the dark for 20 min (or until the standards and samples have developed a blue colour).

NOTE: TMB is stored at 4 °C but should be used at room temperature.

4.4.2.11. Stop the reaction by adding 25 µL stop solution (1 M H_2SO_4) per well and note the color change from blue to yellow.

4.4.2.12. Read the plate at 450 nm absorbance using a microplate reader. Set wavelength correction to 540 nm absorbance to maximize accuracy. Calculate the protein concentrations in the samples from the standard curve produced.

REPRESENTATIVE RESULTS:

Differentiation methodology and progression

Here we present the details of both the methods employed for the generation of vmAstros and the protocols used for their subsequent phenotypic characterization. The method for generation of vmAstros is made up of several distinct differentiation stages, which can be monitored by microscopy and identifying distinct morphological characteristics (**Figure 1A–F**). A feeder-free hiPSC culture (**Figure 1B**) is exposed to specific factors to induce their differentiation toward a neural lineage (LDN193189, SB431542), specifically of the ventral midbrain (CHIR99021, SHH-C24ii). This results in the generation of a culture of vmNPCs, which are morphologically distinct from hiPSCs—the vmNPCs are less rounded than hiPSCs and vmNPCs have an elongated polygonal or triangular shape, typical of neural progenitors (**Figures 1B,C**). The morphological distinction is apparent from day 7–10 onward. When vmNPCs are passaged, similar to hiPSCs, we aim to maintain them as small cell clusters rather than single cells to increase cell survival (**Figure 1D**). However, whereas hiPSCs when passaged quickly form and remain as distinct colonies, vmNPCs readily form a monolayer (**Figure 1C**). From day 20 onward, vmNPCs can be used to generate midbrain dopaminergic neurons (**Figure 1A**), which we have previously published[30,31].

Our strategy to generate vmAstros from the vmNPCs relied on an understanding of the developing embryonic brain, the acquisition of astroglial fate in the embryo, and also how this has been applied to ex vivo neural progenitors and hiPSCs to generate astrocytes[22,23,25,32–37]. Elongated time in culture together with the activation of specific signaling pathways has been demonstrated to be required by mammalian NPCs to recapitulate the timing enabling the shift in neuronal potency toward the astroglial lineage in vitro[6,21–23,32]. Therefore, we used LIF and EGF to support the elongated expansion of the cultures from day 30–90 (**Figure 1A**). Both JAK/STAT signaling downstream of LIF, and EGF signaling are inducers of astroglial identity and also selectively act as mitogens on astroglial progenitors[22,23,25,33,34]. Media components for the culture of vmAPCs are modified from those demonstrated by[22] to support the generation of astrocytes from hiPSCs.

During the EGF/LIF mediated expansion, period cells are referred to as vmAPCs (**Figures 1A,E**). We expect that between days 50 and 90 to culture the vmAPCs in 175 cm^2 tissue culture flasks, passaging at ratios between 1:4 and 1:6 every 4 days, thus enabling rapid expansion of vmAPCs, which can be cryopreserved for future use.

From day 90 onward, vmAstros are generated from vmAPCs via the application of BMP4 in combination with LIF (**Figure 1F**). BMP signaling is required in vivo for mature astrocyte

differentiation and recapitulates this effect in vitro[21,23,37,38]. In the culture flask, mature vmAstros appear larger than vmAPCs (**Figure 1F**).

The protocol detailed here has been carried out over six independent repeats, reproducibly generating vmAstros from the hiPSC line NAS2 and AST23. In addition, the generation of vmNPCs (for producing ventral midbrain dopamine neurons) has been carried out on multiple hiPSC and hESC lines as detailed in[30].

Characterization of vmAstros differentiation and phenotype

The ventral midbrain identity of the vmNPCs was confirmed by co-expression of the neural progenitor marker Musashi1 (MSI1) and the ventral midbrain transcription factor FOXA2 (**Figure 2A**). vmNPCs readily generate midbrain dopamine neurons, which co-express FOXA2 and dopaminergic marker tyrosine hydroxylase (TH) (**Figure 2B**). Expansion of vmNPCs in the presence of EGF and LIF leads to the appearance of vmAPCs (**Figure 2C**). From day 90 onward of the protocol, vmAPCs are exposed to BMP4 in combination with LIF to induce maturation into vmAstros (**Figure 2D**). Immunocytochemistry confirmed co-expression of the ventral midbrain transcription factors LMX1A, LMX1B, and FOXA2 with the astrocyte marker S100β (**Figure 2E–G**). vmAstros also express the mature astrocyte marker GFAP (**Figure 2H**) and the novel marker CD49f, which has been shown to be specific to mature, functional astrocytes[39,40] (**Figure 2I**). Together these results confirm that treatment with BMP4 and LIF induces a mature astrocyte identity, as demonstrated both in vivo and in vitro, and that mature vmAstros maintain the regional ventral midbrain identity acquired in the primary stages of the differentiation protocol[21,37,38] (**Figure 2E–I**).

To confirm that the vmAstros are capable of neuroinflammatory modulation in line with their in vivo counterparts, we characterized their response to cytokine exposure. Exposure of vmAstros to the cytokine IL-1α for 24 h resulted in morphological changes similar to those demonstrated by ex vivo reactive mouse astrocytes[9] (**Figure 2J,K**). Specifically, upon addition of IL-1α, a large proportion of the vmAstros demonstrated a smaller, rounded cell body with multiple projections (**Figure 2K**). To confirm that these changes were representative of a reactive astrocyte phenotype in response to the neuroinflammatory stimuli, we measured the level of IL-6 secreted by the vmAstros. Increased IL-6 secretion is an indicator of reactivity in astrocytes. We measured IL-6 levels by ELISA after a 24 h treatment with IL-1α, which confirmed a large and significant increase in secreted IL-6, thus confirming the vmAstros were demonstrating a reactive phenotype (**Figure 2L**).

FIGURE AND TABLE LEGENDS:

Figure 1: HiPSC differentiation into vmAstros. (**A**) A schematic representation of the optimized protocol to generate vmAstros from hiPSC. The protocol is made up of distinct stages; first a neural, ventral midbrain fate is through dual-SMAD inhibition (with SB431542 and LDN193189) in combination with ventral midbrain patterning molecules (SHH (C24ii) and CHIR99021). vmNPCs proliferate rapidly in the absence of any exogenous mitogens during the vmNPC expansion stage. The addition of BDNF, GDNF, and ascorbic acid promotes survival of vmNPCs, supporting an

increase in cell number. Addition of EGF and LIF sustains proliferation and promotes acquisition of astroglial fate over an extended culture period. After a minimum of 90 days from the initial hiPSC, vmAPCs form mature vmAstros upon exposure to BMP4. (**B–F**) Images of cells as they should appear at different stages in the protocol. hiPSCs and vmNPCs cells are passaged as small clusters, rather than single cells (**C**). Scale bars: B = 500 μm; C = 250 μm; D & E = 200 μm.

Figure 2: Characterization of the phenotype of intermediate cells and vmAstros generated using the described protocol, confirming a ventral midbrain identity. (**A**) Immunocytochemistry demonstrated vmNPCs express the neural progenitor marker MSI1 (red) and the ventral midbrain transcription factor FOXA2 (green). (**B**) vmNPCs are capable of generating midbrain dopamine neurons co-expressing dopaminergic marker tyrosine hydroxylase (TH; red) and ventral midbrain transcription factor FOXA2 (green) (previously published in[30]). (**C**) High magnification phase contrast images show the morphology of vmAPCs compared to (**D**) the mature vmAstros, which have a larger area from nucleus to cell membrane. Immunocytochemistry demonstrated mature vmAstros co-express astrocyte marker S100β and ventral midbrain markers LMX1A (**E**), LMX1B (**F**), and FOXA2 (**G**). (**H,I**) vmAstros express GFAP and CD49f, which are associated with a mature astrocyte phenotype. (**J,L**) Representative images demonstrating the morphology of untreated cultures of vmAstros (**J**), compared to those exposed to IL-1α for 24 h (**K**). Exposure to IL-1α resulted in clear morphological changes **(K)**. **(L)** In response to IL-1α, vmAstros significantly increased secretion of IL-6, indicating vmAstros are generating a reactive phenotype in response to neuroinflammatory stimuli (n = 3 independent experiments, SEM, unpaired *t*-test p = 0.0227). All immunofluorescence images were taken on a confocal microscope. Scale bars: A, B, I = 50 μm; C, D = 100 μm; E, F = 25 μm; G,H = 100 μm.

DISCUSSION:

This method for the generation of vmAstros from hiPSCs is highly efficient, generating pure cultures of vmAstros, and being reproducible for the generation of vmAstros from different hiPSC lines. This protocol was developed around the recapitulation of the developmental events required in the embryo to correctly pattern the developing midbrain and generate astrocytes and comprises three defined stages: 1) neural ventral midbrain induction to generate vmNPCs, 2) generation and expansion of vmAPCs, and finally 3) maturation of vmAstros.

In our previous published work, we highlighted the importance of optimizing the concentrations of CHIR99021 and SHH(C24ii) for each hiPSC line used to generate vmNPCs, to ensure optimal expression of ventral midbrain markers[30,31]; 200 ng/mL SHH (C24ii) and 0.8 μM CHIR99021 yields consistently reproducible results over multiple hiPSC lines. However, 300 ng/mL SHH (C24ii) and 0.6 μM CHIR99021 can be more efficacious for particular hiPSC lines but can also affect cell survival[30,31]. Therefore, optimization by the user is recommended.

In developing this protocol for the generation of vmAPCs, it was apparent that cell density is critical at all stages. In the vmNPC induction stage, cell density must remain high to support cell survival, as vmNPC density below 75% leads to the death of vmNPCs in large numbers. The rate of proliferation of the vmNPCs is dependent on the rate of proliferation of the parent hiPSC

culture and does vary between lines; however, to maintain a proliferative population, vmNPC density must remain high. Therefore, we recommend that vmNPCs are passaged at conservative ratios until the user has optimized the passaging regime. In contrast vmAPCs should be passaged at high ratios, achieving a cell density of around 30-40% after passaging, and passaging as soon as the cells are confluent. We found in our preliminary experiments that maintaining vmAPCs at very high confluency leads to greater heterogeneity in the resulting vmAstros as indicated by varied morphology expression of astrocyte marker GFAP (data not shown). Micrographs of appropriate cell densities are included in this protocol for reference.

Both the vmNPCs and vmAPCs are highly proliferative, generating large number of cells from a relatively small starting population of iPSCs. For example, we usually begin this protocol with a single 10 cm^2 dish of iPSCs and when we reach day 60, we would expect to culture the APCs in 175 cm^2 flasks, with each passage generating 4-6 new flasks and this rate of expansion would continue until day 90. Extrapolating from this, at minimum we would have the ability to generate up to 4,000 flasks of vmAPCs. We cryopreserve the vmAPCs throughout this expansion period and thus can generate a large cryobank of cells for future generation of mature vmAstros. This is extremely advantageous as it enables high-throughput analysis required for applications such as drug screening.

The unique aspect of this protocol is the midbrain identity of the resulting vmAstros. In the brain, specific regional astroglial populations, similar to their neuronal counterparts, possess specific characteristics[25,26]. A major focus of Parkinson's research is the involvement of astroglial cells in neuroinflammation and how this influences disease progression. Neuroinflammation is present in early Parkinson's and many other injury or disease scenarios[12]. As part of the neuroinflammatory response, astrocytes transform in an attempt to protect neurons from damage—this is referred to as the "reactive astrocyte". However, reactive astrocytes are themselves neurotoxic in chronic diseases such as Parkinson's[9,11]. In animal and in vitro models of Parkinson's, reactive astroglial mediated neuroinflammation is a catalyst for neurotoxic α-synuclein pathology and neurodegeneration[9,14,41–43]. Therefore, we created an in vitro neuroinflammatory environment by treating vmAstros with pro-inflammatory cytokines IL-1α or IL-1β. In response, the vmAstros demonstrated significant morphological changes and we saw a significant increase in secretion of IL-6, which is also elevated in Parkinson's and is widely used as a measure of astrocyte reactivity.

In conclusion, this protocol provides a reproducible and efficient method to generate large numbers of hiPSC-derived vmAstros, which demonstrate a phenotype that parallels their in vivo counterparts in the ventral midbrain. This protocol is therefore highly applicable to high-throughput applications such as drug screening, which require large numbers of human cells. Recent work has highlighted the role of neuroinflammation in Parkinson's diseases, and how pharmacological targeting of astroglia influences neuroinflammation, which in turn modulates disease pathology[11]. As demonstrated, the vmAstros generated with this protocol are appropriately responsive to neuroinflammatory stimulation, providing a comprehensive cellular model with which to study astroglial involvement in Parkinson's disease.

ACKNOWLEDGMENTS:

This work was funded by a Parkinson's UK project grant (G-1402) and studentship. The authors gratefully acknowledge the Wolfson Bioimaging Facility for their support and assistance in this work.

DISCLOSURES:

The authors have nothing to disclose.

REFERENCES:

1. Poewe, W. et al. Parkinson disease. *Nature Reviews Disease Primers*. **3**, 17013 (2017).
2. Lees, A. J., Hardy, J., Revesz, T. Parkinson's disease. *Lancet*. **373**, 2055–2066 (2009).
3. Braak, H. et al. Staging of brain pathology related to sporadic Parkinson's disease. *Neurobiology of Aging*. **24**, 197–211 (2003).
4. Booth, H. D. E., Hirst, W. D., Wade-Martins, R. The role of astrocyte dysfunction in Parkinson's disease pathogenesis. *Trends in Neurosciences*. **40**, 358–370 (2017).
5. Lindstrom, V. et al. Extensive uptake of alpha-synuclein oligomers in astrocytes results in sustained intracellular deposits and mitochondrial damage. *Molecular and Cellular Neuroscience*. **82**, 143–156 (2017).
6. Crompton, L. A., Cordero-Llana, O., Caldwell, M. A. Astrocytes in a dish: Using pluripotent stem cells to model neurodegenerative and neurodevelopmental disorders. *Brain Pathology*. **27**, 530–544 (2017).
7. di Domenico, A. et al. Patient-specific iPSC-derived astrocytes contribute to non-cell-autonomous neurodegeneration in Parkinson's disease. *Stem Cell Reports*. **12**, 213–229 (2019).
8. Zhang, Y., Barres, B. A. Astrocyte heterogeneity: an underappreciated topic in neurobiology. *Current Opinions in Neurobiology*. **20**, 588–594 (2010).
9. Liddelow, S. A. et al. Neurotoxic reactive astrocytes are induced by activated microglia. *Nature*. **541**, 481–487(2017).
10. Liddelow, S. A., Barres, B. A. Reactive astrocytes: production, function, and therapeutic Potential. *Immunity*. **46**, 957–967 (2017).
11. Yun, S. P. et al. Block of A1 astrocyte conversion by microglia is neuroprotective in models of Parkinson's disease. *Nature Medicine*. **24**, 931–938 (2018).
12. Stokholm, M. G. et al. Assessment of neuroinflammation in patients with idiopathic rapid-eye-movement sleep behaviour disorder: a case-control study. *The Lancet Neurology*. **16**, 789–796 (2017).
13. Williams-Gray, C. H. et al. Serum immune markers and disease progression in an incident Parkinson's disease cohort (ICICLE-PD). *Movement Disorders*. **31**, 995–1003 (2016).
14. Gelders, G., Baekelandt, V., Van der Perren, A. Linking neuroinflammation and neurodegeneration in Parkinson's disease. *Journal of Immunology Research*. **2018**, 4784268 (2018).
15. Hall, S. et al. Cerebrospinal fluid concentrations of inflammatory markers in Parkinson's disease and atypical parkinsonian disorders. *Scientific Reports*. **8**, 13276 (2018).
16. Zamanian, J. L. et al. Genomic analysis of reactive astrogliosis. *Journal of Neuroscience*. **32**, 6391–6410 (2012).

17. Clarke, B. E. et al. Human stem cell-derived astrocytes exhibit region-specific heterogeneity in their secretory profiles. *Brain*. **143** (10), e85 (2020).
18. Sevenich, L. Brain-resident microglia and blood-borne macrophages orchestrate central nervous system inflammation in neurodegenerative disorders and brain cancer. *Frontiers in Immunology*. **9**, 697 (2018).
19. Friedman, B. A. et al. Diverse brain myeloid expression profiles reveal distinct microglial activation states and aspects of Alzheimer's disease not evident in mouse models. *Cell Reports*. **22**, 832–847(2018).
20. Viti, J., Feathers, A., Phillips, J., Lillien, L. Epidermal growth factor receptors control competence to interpret leukemia inhibitory factor as an astrocyte inducer in developing cortex. *Journal of Neuroscience*. **23**, 3385–3393 (2003).
21. Nakashima, K., Yanagisawa, M., Arakawa, H., Taga, T. Astrocyte differentiation mediated by LIF in cooperation with BMP2. *FEBS Letters*. **457**, 43–46 (1999).
22. Serio, A. et al. Astrocyte pathology and the absence of non-cell autonomy in an induced pluripotent stem cell model of TDP-43 proteinopathy. *Proceedings of the National Academy of Sciences of the United States of America*. **110**, 4697–4702 (2013).
23. Gupta, K. et al. Human embryonic stem cell derived astrocytes mediate non-cell-autonomous neuroprotection through endogenous and drug-induced mechanisms. *Cell Death and Differentiation*. **19**, 779–787 (2012).
24. Krencik, R., Ullian, E. M. A cellular star atlas: using astrocytes from human pluripotent stem cells for disease studies. *Frontiers in Cellular Neuroscience*. **7**, 25 (2013).
25. Krencik, R., Weick, J. P., Liu, Y., Zhang, Z.-J., Zhang, S.-C. Specification of transplantable astroglial subtypes from human pluripotent stem cells. *Nature Biotechnology*. **29**, 528–534 (2011).
26. Xin, W. et al. Ventral midbrain astrocytes display unique physiological features and sensitivity to dopamine D2 receptor signaling. *Neuropsychopharmacology*. **44**, 344–355 (2019).
27. Devine, M. J. et al. Parkinson's disease induced pluripotent stem cells with triplication of the alpha-synuclein locus. *Nature Communications*. **2**, 440 (2011).
28. Chen, Y. et al. Engineering synucleinopathy-resistant human dopaminergic neurons by CRISPR-mediated deletion of the SNCA gene. *European Journal of Neuroscience*. **49**, 510–524 (2019).
29. Crompton, L. A. et al. Stepwise, non-adherent differentiation of human pluripotent stem cells to generate basal forebrain cholinergic neurons via hedgehog signaling. *Stem Cell Research*. **11**, 1206–1221 (2013).
30. Stathakos, P. et al. A monolayer hiPSC culture system for autophagy/mitophagy studies in human dopaminergic neurons. *Autophagy*. 1–17 (2020).
31. Stathakos, P. et al. Imaging autophagy in hiPSC-derived midbrain dopaminergic neuronal cultures for Parkinson's disease research. *Methods in Molecular Biology*. **1880**, 257–280 (2019).
32. Bilican, B. et al. Mutant induced pluripotent stem cell lines recapitulate aspects of TDP-43 proteinopathies and reveal cell-specific vulnerability. *Proceedings of the National Academy of Sciences of the United States of America*. **109**, 5803–5808 (2012).

33. Cordero-Llana, O. et al. Clusterin secreted by astrocytes enhances neuronal differentiation from human neural precursor cells. *Cell Death and Differentiation*. **18**, 907–913 (2011).
34. Morrow, T., Song, M. R., Ghosh, A. Sequential specification of neurons and glia by developmentally regulated extracellular factors. *Development*. **128**, 3585–3594 (2001).
35. Namihira, M. et al. Committed neuronal precursors confer astrocytic potential on residual neural precursor cells. *Developmental Cell*. **16**, 245–255 (2009).
36. Ochiai, W., Yanagisawa, M., Takizawa, T., Nakashima, K., Taga, T. Astrocyte differentiation of fetal neuroepithelial cells involving cardiotrophin-1-induced activation of STAT3. *Cytokine*. **14**, 264–271 (2001).
37. Nakashima, K., Yanagisawa, M., Arakawa, H. Synergistic signaling in fetal brain by STAT3-Smad1 complex bridged by p300. *Science*. **284** (5413) 479–482 (1999).
38. Nakashima, K. et al. Developmental requirement of gp130 signaling in neuronal survival and astrocyte differentiation. *Journal of Neuroscience*. **19**, 5429–5434 (1999).
39. Barbar, L. et al. CD49f is a novel marker of functional and reactive human iPSC-derived astrocytes. *Neuron*. **107**, 436–453 e412 (2020).
40. Barbar, L., Rusielewicz, T., Zimmer, M., Kalpana, K., Fossati, V. Isolation of human CD49f(+) astrocytes and in vitro iPSC-based neurotoxicity assays. *STAR Protocols*. **1**, 100–172 (2020).
41. Gao, H. M. et al. Neuroinflammation and alpha-synuclein dysfunction potentiate each other, driving chronic progression of neurodegeneration in a mouse model of Parkinson's disease. *Environmental Health Perspectives.* **119**, 807–814 (2011).
42. Gao, H. M. et al. Neuroinflammation and oxidation/nitration of alpha-synuclein linked to dopaminergic neurodegeneration. *Journal of Neuroscience*. **28**, 7687–7698 (2008).
43. Horvath, I. et al. Co-aggregation of pro-inflammatory S100A9 with alpha-synuclein in Parkinson's disease: ex vivo and in vitro studies. *Journal of Neuroinflammation*. **15**, 172 (2018).

Figure 1

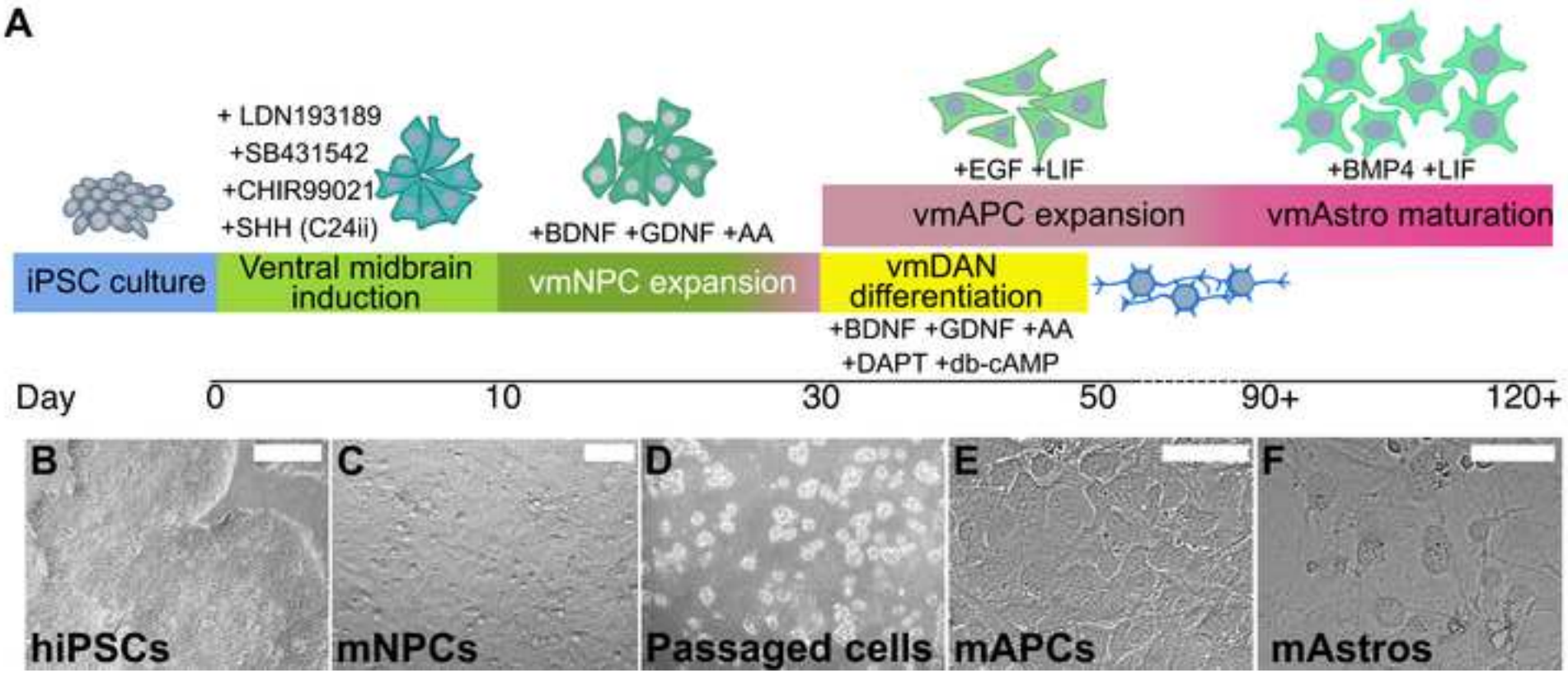

Figure 2

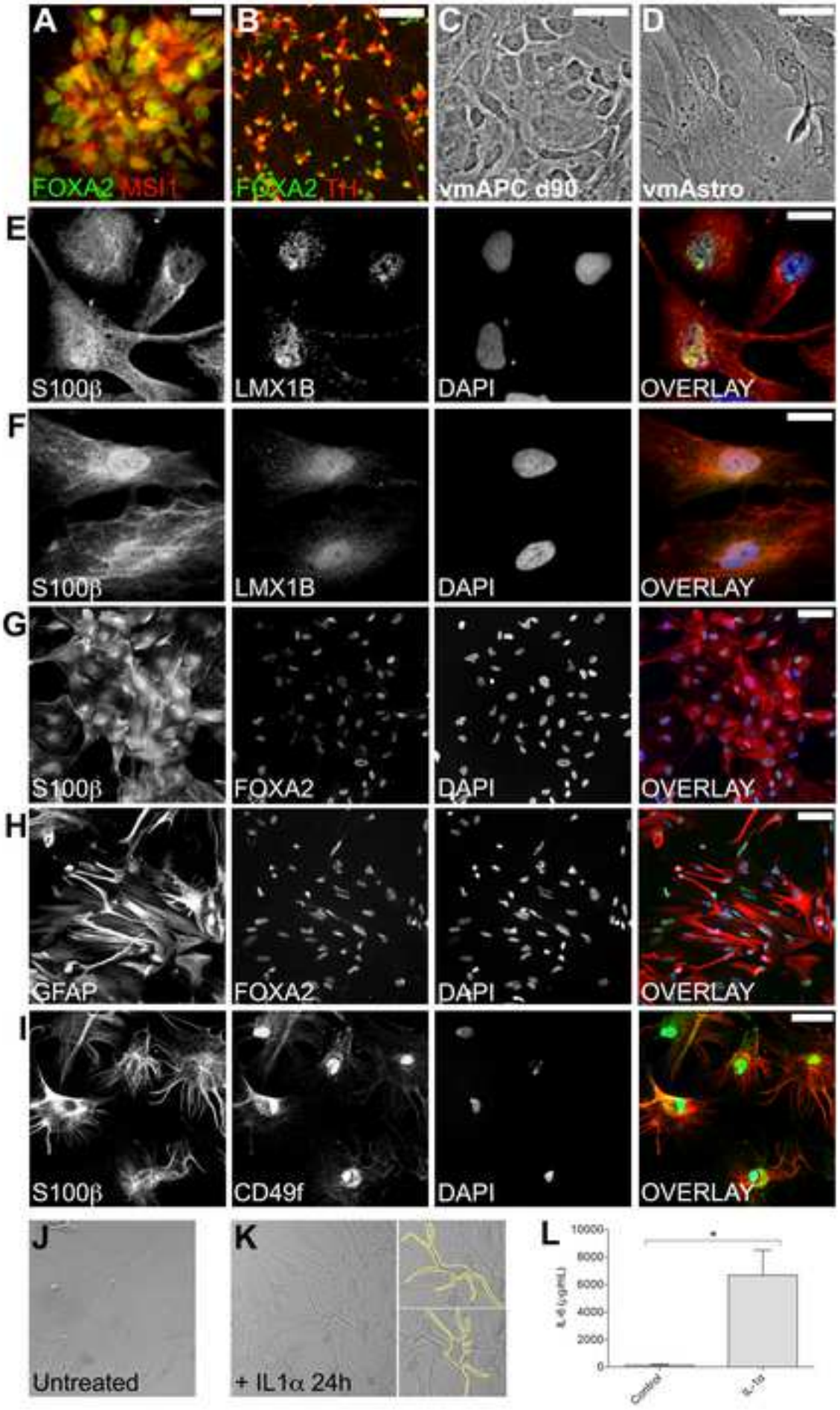

Table of Materials

Click here to access/download;Table of Materials;JOVE table of materials Revision.xls

Reagents	Company	Catalogue Number
0.2M Tris-Cl (pH 8.5)	n/a	n/a
0.5M EDTA, PH 8	ThermoFisher	15575-020
1,4-diazabicylo[2.2.2]octane (DABCO)	Sigma	D27802-
13 mm coverslips	VWR	631-0149
2-Mercaptoethanol (50 mM)	ThermoFisher	31350010
Accutase	ThermoFisher	13151014
Advanced DMEM/F12	ThermoFisher	12634010
Ascorbic acid	Sigma	A5960
B27 Supplement	ThermoFisher	17504-044
BSA	Sigma	5470
Cell freezing media	Sigma	C2874
Cell freezing vessel	Nalgene	5100-0001
CHIR99021	Axon Medchem	1386
Cryovials	Sigma	CLS430487
DAPI	Sigma	D9542
DMEM/F12 + Glutamax	ThermoFisher	10565018
Dulbeccos-PBS (D-PBS without Mg or Ca)	ThermoFisher	20012
E8 Flex medium kit	ThermoFisher	A2858501
Formaldehyde (36% solution)	Sigma	47608
Geltrex	ThermoFisher	A1413302
Glutamax	ThermoFisher	35050038
Glycerol	Sigma	G5516
Human BDNF	Peprotech	450-02
Human BMP4	Peprotech	120-05
Human EGF	Peprotech	AF-100-15
Human GDNF	Peprotech	450-10
Human insulin solution	Sigma	I9278
Human LIF	Peprotech	300-05
IL-6 ELISA kit	Biotechne	DY206
Isopropanol	Sigma	I9516-4L
LDN193189	Sigma	SML0559
Mowiol 40-88	Sigma	324590
N2 Supplement	ThermoFisher	17502048
NEAA	ThermoFisher	11140035
Neurobasal media	ThermoFisher	21103049

Normal Goat serum	Vector Labs	S-1000-20
Revitacell	ThermoFisher	A2644501
SB431542	Tocris	1614
SHH-C24ii	Biotechne	1845-SH-025
Tris-HCl	Sigma	PHG0002
Triton-X	Sigma	X100
Tween-20	Sigma	P7949
Vitronectin	ThermoFisher	A14700

Antibodies for immunocytochemistry	**Company**	**Catalogue Number**
Antibody against S100b	Sigma	SAB4200671
Antibody against FOXA2	SCBT	NB600501
Antibody against LMX1A	ProSci	7087
Antibody against LMX1A	Millipore	AB10533
Antibody against LMX1B	Proteintech	18278-1-AP
Antibody against GLAST	Proteintech	20785-1-AP
Antibody against GFAP	Dako	Z0334
Antibody against CD49f	Proteintech	27189-1-AP
Antibody against MSI1	Abcam	ab52865
Alexa Fluor 488 Goat Anti-Rabbit	ThermoFisher	A32731
Alexa Fluor 488 Goat Anti-Mouse	ThermoFisher	A32723
Alexa Fluor 568 Goat Anti-Rabbit	ThermoFisher	A11036
Alexa Fluor 488 Goat Anti-Mouse	ThermoFisher	A11031

Comments	
Made up from Tris base and plus HCl	
1:1000 in D-PBS to 0.5 mM final	
25 mg/ml in Mowiol mounting solution	
Has 1x NEAA but we add to final concentration of 2x (0.2 mM)	
200 mM stock, 1:1000 to 200 □M final	
50x stock	
Cryostor CS10	
0.8 mM stock, 1:1000 dilution to 0.8 □M final	
1 mg/ml, 1:10,000 to 100ng/ml final (in PBS)	
pH 7.4	
1:100 or 1:400 in ice-cold DMEM/F12	
2 mM stock (1:200 in N2B27, 1:100 in ASTRO media to 20□□M final)	
20 □g/ml stock, 1:1000 to 20 ng/ml final	
20 □g/ml stock, 1:1000 to 20 ng/ml final	
20 □g/ml stock, 1:1000 to 20 ng/ml final	
20 □g/ml stock, 1:1000 to 20 ng/ml final	
10 mg/ml stock, 1:2000 to 5 □g/ml final	
20 □g/ml stock, 1:1000 to 20 ng/ml final	
For filling Mr Frosty cryostorage vessel	
100□□M stock, 1:10,000 dilution to 10 nM final	
100x stock	
10 mM stock, 1:100 to 0.1 mM final	

100x stock, 1:100 to 1x final	
10 mM stock, 1:1000 dilution to 10 □M final	
200 □g/ml stock, 1:1000 to 200 ng/ml final	
1:50 in D-PBS	

Host species	**Dilution Factor**
Mouse	1:200
Mouse	1:50
Rabbit	1:300
Rabbit	1:2000
Rabbit	1:300
Rabbit	1:300
Rabbit	1:400
Rabbit	1:100
Rabbit	1:400
Goat	1:500
Goat	1:500
Goat	1:500
Goat	1:500

0.2M Tris-(	n/a	n/a	Made up from Tris base and plus HCl
0.5M EDTA	ThermoFis	15575-02(	1:1000 in D-PBS to 0.5 mM final
1,4-diazabi	Sigma	D27802-	25 mg/ml in Mowiol mounting solution
13 mm cov	VWR	631-0149	
2-Mercapt	ThermoFis	31350010	
Accutase	ThermoFis	13151014	
Advanced	ThermoFis	12634010	Has 1x NEAA but we add to final concentration of 2x (0.2 mM)
Ascorbic a(	Sigma	A5960	200 mM stock, 1:1000 to 200 □M final
B27 Supple	ThermoFis	17504-044	50x stock
BSA	Sigma	5470	
Cell freezir	Sigma	C2874	Cryostor CS10
Cell freezir	Nalgene	5100-0001	
CHIR99021	Axon Med(	1386	0.8 mM stock, 1:1000 dilution to 0.8 □M final
Cryovials	Sigma	CLS430487	
DAPI	Sigma	D9542	1 mg/ml, 1:10,000 to 100ng/ml final (in PBS)
DMEM/F1	ThermoFis	10565018	
Dulbeccos-	ThermoFis	20012	pH 7.4
E8 Flex me	ThermoFis	A2858501	
Formaldeh	Sigma	47608	
Geltrex	ThermoFis	A1413302	1:100 or 1:400 in ice-cold DMEM/F12
Glutamax	ThermoFis	35050038	2 mM stock (1:200 in N2B27, 1:100 in ASTRO media to 20□□M final)
Glycerol	Sigma	G5516	
Human BD	Peprotech	450-02	20 □g/ml stock, 1:1000 to 20 ng/ml final
Human BM	Peprotech	120-05	20 □g/ml stock, 1:1000 to 20 ng/ml final
Human EG	Peprotech	AF-100-15	20 □g/ml stock, 1:1000 to 20 ng/ml final
Human GD	Peprotech	450-10	20 □g/ml stock, 1:1000 to 20 ng/ml final
Human ins	Sigma	I9278	10 mg/ml stock, 1:2000 to 5 □g/ml final
Human LIF	Peprotech	300-05	20 □g/ml stock, 1:1000 to 20 ng/ml final
IL-6 ELISA	Biotechne	DY206	
Isopropan(	Sigma	I9516-4L	For filling Mr Frosty cryostorage vessel
LDN19318	Sigma	SML0559	100□□M stock, 1:10,000 dilution to 10 nM final
Mowiol 40	Sigma	324590	
N2 Supple	ThermoFis	17502048	100x stock
NEAA	ThermoFis	11140035	10 mM stock, 1:100 to 0.1 mM final
Neurobasa	ThermoFis	21103049	
Normal Go	Vector Lab	S-1000-20	
Revitacell	ThermoFis	A2644501	100x stock, 1:100 to 1x final
SB431542	Tocris	1614	10 mM stock, 1:1000 dilution to 10 □M final
SHH-C24ii	Biotechne	1845-SH-0	200 □g/ml stock, 1:1000 to 200 ng/ml final
Tris-HCl	Sigma	PHG0002	
Triton-X	Sigma	X100	
Tween-20	Sigma	P7949	
Vitronectir	ThermoFis	A14700	1:50 in D-PBS

Table 1. Reagent preparation for hiPSC differentiation into ventral midbrain astroc

Cell culture media	
N2B27 media	
	Neurobasal media supplemented with 1
	DMEM/F12 + glutamax
	Non-essential amino acids
	β–mercaptoethanol
	B27
	N2
	Human Insulin solution (10 mg/mL)
ASTRO media (based on[22])	
	Advanced DMEM/F12
	Non-essential amino acids (in addition to
	Glutamax
	N2
	B27

Addtional culture media additives		
Reagent	**Supplied as**	**Stock concentratio**
Ascorbic acid	powder	200 mM
BDNF	lyophilized powder	20 µg/mL
BMP4	lyophilized powder	20 µg/mL
EGF	lyophilized powder	20 µg/mL
GDNF	lyophilized powder	20 µg/mL
LDN193189	lyophilized powder	1 mM
LIF	lyophilized powder	20 µg/mL
SB431542	lyophilized powder	10 mM
SHH-C24ii	lyophilized powder	200 µg/mL

cytes (vmAstros)

	% of final
% glutamax	48.675
	48.675
	1
	0.1
	1
	0.5
	0.05
	96.6
o those in Advanced DMEM/F12)	1
	1
	1
	0.4

Reconstitute in	Details	Storage
filter sterilized water	0.0284 mL per 1 mg	Aliquot and store at -20 °C
filter sterilized D-PBS with 0.1% BSA	10 ml per mg	Aliquot and store at -20 °C
filter sterilized D-PBS with 0.1% BSA	10 ml per mg	Aliquot and store at -20 °C
filter sterilized D-PBS with 0.1% BSA	10 ml per mg	Aliquot and store at -20 °C
filter sterilized D-PBS with 0.1% BSA	10 ml per mg	Aliquot and store at -20 °C
DMSO	2.085 mL per mg	Aliquot and store at -20 °C
filter sterilized D-PBS with 0.1% BSA	10 ml per mg	Aliquot and store at -20 °C
DMSO	0.239 mL per mg	Aliquot and store at -20 °C
filter sterilized D-PBS with 0.1% BSA	1 ml per mg	Aliquot and store at -20 °C

m

Final concentraion in media
200 μM
20 ng/mL
20 ng/mL
20 ng/mL
20 ng/mL
100 nM
20 ng/mL
10 μM
20 ng/mL

Response to reviewers' comments for JOVE article submission JoVE62095

Dear reviewers,

Firstly, we would like to thank you for your valuable feedback relating to our article, and the positive, constructive comments provided. We have tried to address your questions and concerns in the following document, and with the required revisions to the manuscript.

We think it is important to state that submission JoVE62095 outlines the protocols that we have developed and used in our current and ongoing research, data from which will be presented in a separate manuscript that is in preparation. We envisaged that JoVE62095 and our research publications would be submitted at around the same time; however, due to the impact of COVID-19, we are still completing final experiments for the other manuscript, which we will submit early 2021. Therefore, many of the reviewers' comments (below) are answered using data that are to form part of our manuscript in preparation, and we do not wish these data to contribute to the JoVE62095 submission. Therefore, we request that the editor and reviewers consider these unpublished data as evidence of efficacy with respect to our protocols. Publication in the near future of a manuscript containing extensive data based on these protocols will nicely synergise with JoVE62095, which will of course be fully cited.

All changes to the manuscript are highlighted in cyan.

Reviewers' comments:

Reviewer #1:

Reviewer Comments:

The method paper by Crompton et al. describes the generation of human midbrain astrocytes from human iPSCs. Though the protocol is clearly described, there are several concerns related, especially to midbrain astrocytes' characterization and partly also to the distinct steps of differentiation.

General question:

1) Both in abstracts and introduction, the authors bring attention to the inflammation, but astrocytes are not the primary cells responsible for it. The connection with microglia is completely missing from this content and should be explained. Do microglia play a role as well in inflammation seen as an early event in Parkinson´s disease?

The reviewer is correct - the omission of any comment on microglia from the manuscript was an oversight. It is the relationship between microglia and astrocytes that is particularly important in Parkinson's disease. It has been demonstrated that pharmacological inhibition of the ability of microglia to 'activate' astrocytes halts disease pathology (Yun, Kam et al. 2018). As suggested, we have altered the abstract (lines 42-44) and introduction (lines 72-92) to introduce the significant role of microglia in this setting.

More specific questions and comments:

2) The fibroblast growth factor 8 (FGF8) is a morphogenic patterning molecule that is commonly used for the derivation of midbrain dopaminergic neurons and midbrain organoids. In the presented protocol, this molecule has been omitted. What were the essentials for this? Did the authors try to derive the midbrain astrocytes with and without this molecule?

We acknowledge that FGF8 is used in numerous hiPSC differentiation protocols for the generation of ventral midbrain dopamine neurons to mimic FGF signalling required for patterning the embryonic midbrain. For these reasons we have also previously investigated whether addition of FGF8 influences generation of ventral midbrain progenitors and dopamine neurons, finding that in terms of the generation of ventral midbrain dopamine neurons, the inclusion of FGF8 had no effect (Stathakos, Jimenez-Moreno et al. 2020). The early stages of our protocol are based closely on that published by Kriks et al., 2011, who also demonstrated that FGF8 did not have a significant effect on the induction of midbrain floor plate. In fact CHIR99021 used in combination with SHH had the greatest effect (Kriks, Shim et al. 2011). Indeed, based on the findings by Kriks et al., there have been multiple published examples of protocols that differentiate midbrain floor plate precursors towards ventral midbrain dopamine neurons. Furthermore, we have demonstrated that the vmNPCs generated in the current protocol, and from which we derive the vmAstros, express LMX1A, LMX1B, and FOXA2 (Stathakos, Jimenez-Moreno et al. 2020), and we also show these

transcription factors are also present in the vmAstros (fig 2 E-G of submitted manuscript). In addition, we have data demonstrating sustained expression of midbrain marker *EN1* at every stage of our protocol and also in the mature vmAstros (Figure R1). These data are for the reviewers' attention only, as they are to be be published on a manuscript currently in preparation, which focuses on the characterization and neuroinflammatory response of hiPSC-derived vmAstros (see note above).

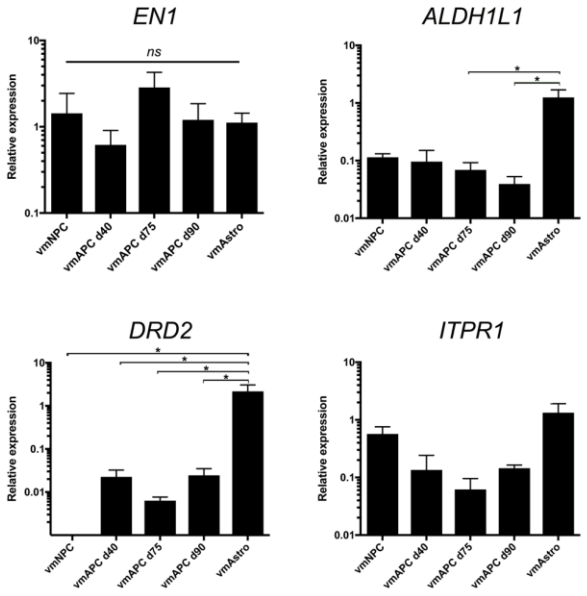

Figure R1. qRT-PCR analysis demonstrating the relative expression of the *EN1*, *ALDH1L1*, *DRD2* and *ITPR1* at various stages of our vmAstro differentiation protocol. The ventral midbrain transcription factor *EN1* shows sustained expressed at every stage of differentiation and is maintained in the mature vmAstrocytes. Expression of the astrocyte marker *ALDH1L1*, and the dopamine receptor D2 gene *DRD2*, which is involved in the functioning of vmAstros in the mature rodent brain, are significantly higher in vmAstros compared to vmAPCs. This indicates exposure to BMP4 and hLIF in the maturation stage of our protocol results changes in gene expression associated with mature astrocytes in the ventral midbrain. In addition, *ITPR1*, a gene enriched in vmAstros in the mouse ventral midbrain is also expressed in the hiPSC-derived vmAstros differentiated using the protocol detailed in the manuscript, further verifying the ventral midbrain astrocyte phenotype.

3) Figure 1 illustrates hiPSCs differentiation into vm astrocytes. In the first stage, vmNPC are produced and expanded. The molecules like BDNF, GDNF, and AA are used for neuronal stage and neurons' maturation, not for expanding neuroprogenitors! This is most likely a mistake as the image above shows a rosette-like structure, not a neuronal one!

Thank you to the reviewer for highlighting this. We are aware that BDNF, GDNF and ascorbic acid are frequently used to support the differentiation and survival of neurons during and after their differentiation. However, we make no claim that in our protocol these are the factors driving proliferation of the vmNPCs, although at this stage of the protocol, the vmNPCs do proliferate at a significant rate, just as they do in the preceding ventral midbrain induction stage. Therefore, we chose to refer to this as the vmNPC expansion stage of the protocol. The first stages of the protocol were initially optimised for the generation of vmDANs (Stathakos, Jimenez-Moreno et al. 2020), and so a major driver for protocol development was the production of large numbers of vmNPCs (and subsequently vmDANs) consistently from every differentiation attempt. Other published protocols proceed directly from the induction phase to neuronal differentiation(Kriks, Shim et al. 2011). However, in our hands, vmNPCs can be expanded up to day 40-50, whilst continuing to readily generate vmDANs upon the addition of DAPT and cAMP. We propose that together these factors support the survival of vmNPCs, rather than acting as potent mitogens, as in agreement with general literature on the role of these factors. GDNF has been shown to promote proliferation of neural and other cells types, whilst having an anti-apoptotic affect, and we therefore suggest that it is this pro-survival affect alongside continuing proliferation that leads to increase in cell numbers (Cortes, Carballo-Molina et al. 2017). We have inserted a sentence in the manuscript to acknowledge this (lines 441-442). We also acknowledge your suggestion that in Figure 1 rosettes are more representative of the induction phase, and we have therefore edited this accordingly. We have also referred to the use of GDNF and BDNF and ascorbic acid in the legend for figure 1.

4) Derived astrocytes are very poorly characterized except for showing the markers representing the midbrain. The staining for at least the following markers has to be shown: glial-fibrillar acidic protein (GFAP) and aquaporin 4 (AQP4). More further, astrocytes' functionality is provided only after the treatment of astrocytes with a low dose of IL-1a or IL-1b. While according to figure legend 2 (J), astrocytes exposed to IL-1b significantly increased release of IL-6, the figure shows the response after the IL-1a exposure.....please show the response after both treatments. Also, indicate which morphological changes correspond to which interleukin exposure in figure 2 (I). Regarding the functionality tests of astrocytes - glucose and glutamate uptake need to be presented.

In response to this point, we would like to reiterate that we are currently preparing a manuscript which focuses on the characterization of the hiPSC-derived vmAstros and their reactive phenotype in response to neuroinflammation, in which we will report in depth characterisations of vmAstro functionality. The data shown in Figure R1 (for reviewers' eyes only) provide some additional characterisation, including evidence that exposure to BMP4 in combination with LIF in the maturation stage of the protocol led to a significant increase in expression of *ALDH1L1,* associated with a mature astrocyte phenotype, and *DRD2,* homologues of which are crucial to the function of ventral midbrain astrocytes in the rodent brain (Cahoy, Emery et al. 2008, Xin, Schuebel et al. 2019) (Figure R1). Similarly, we demonstrate expression of *ITPR1*, the homologue of which is highly enriched in adult rodent ventral midbrain astrocytes, compared to those of the hippocampus or cortex (Xin, Schuebel et al. 2019) (Figure R1). In addition, as suggested by the reviewer, we have now included images in figure 2 to demonstrate specific expression of GFAP alongside and the novel mature astrocyte marker CD49f (Barbar, Jain et al. 2020, Barbar, Rusielewicz et al. 2020)(Figure 2I).
In response to astrocyte functionality, we have incomplete data which will be published in our upcoming manuscript that demonstrate changes in gene expression associated with a reactive phenotype in response to neuroinflammation, phagocytosis of alpha-synuclein and neuronal debris, and we are currently carrying out calcium signalling looking for responses to specific stimuli including glutamate. For the reviewers we have included a small selection of this data in Figure R2 as evidence that our protocol generates mature, functional ventral midbrain astrocytes from hiPSCs.
The inclusion of IL1α and IL1β in the original manuscript was in fact a mistake with the editing and we are very grateful to the reviewer for highlighting this. We have revised the figure (Figure 2 J-L) to make the morphological changes in the vmAstros clearer and the data is all based on the exposure of vmAstros to IL1α only.

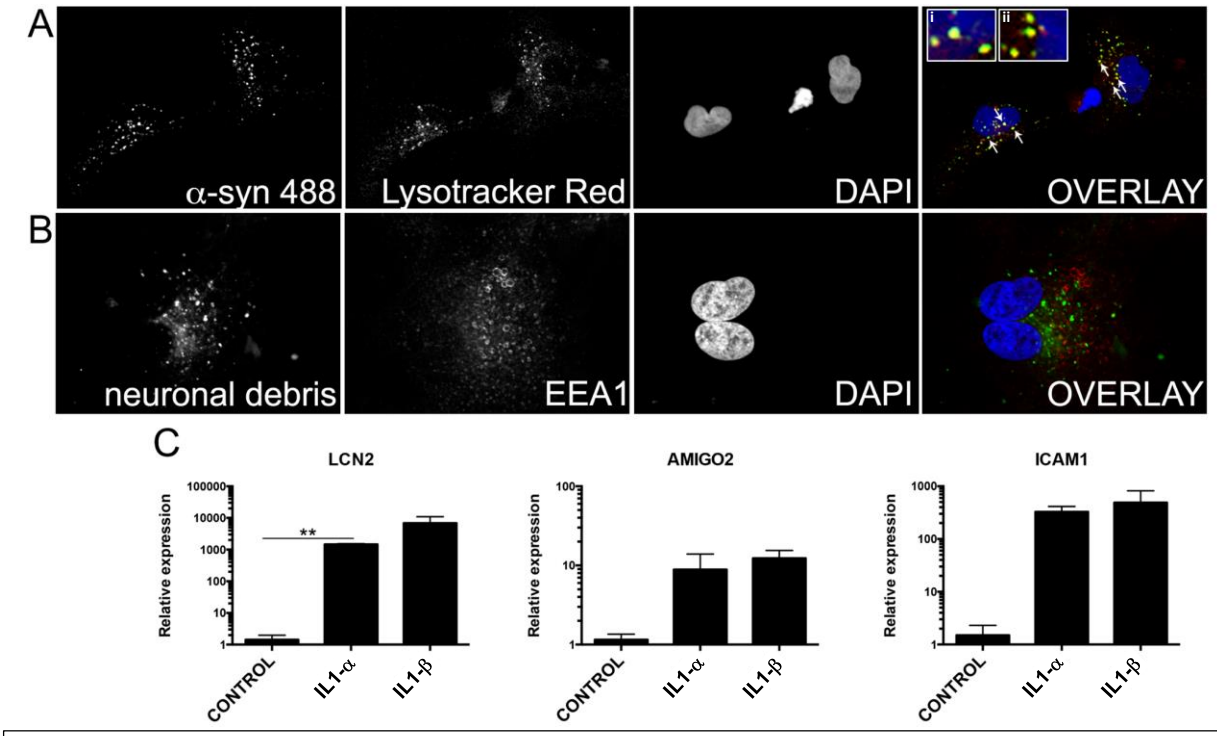

Figure R2 (A) vmAstros internalize fluorescently labelled α-synuclein. After 24h co-staining with lysotracker red demonstrated colocalization with α-synuclein, demonstrating its presence within lysosomes (indicated by arrowheads and at higher magnification in panels I and ii. This colocalisation demonstrating α-synuclein in the lysosomal pathway. (B) vmAstros phagocytose fluorescently labelled debris from human apoptotic neurons. After 18h of exposure the debris can be visualized as distinct puncta within the vmAstros. Co-staining for early endosome antigen EEA1 demonstrated a distinct patterning of localization suggesting that after 18h the phagocytosed debris is no longer within endosomes. We are currently investigating the timing of this phagocytosis and subsequent processing of the internalized α-synuclein and neuronal debris. (C) qRT-PCR analysis demonstrating the relative expression of *LCN2*, *AMIGO2* and *ICAM1* in untreated vmAstros compared to vmAstros exposed to either IL1α and IL1β for 24h. Expression of these genes increase in response to neuroinflammatory stimuli in rodent astrocytes in vitro, and these changed are indicative of astrocyte reactivity.

5) The authors point out that the vm astrocytes were derived from two hiPSC lines. Were these obtained from healthy donors or PD patients?The information should be added there. Also, for the result part, n=3, can you explain what does it mean? How many times was the assay repeated, and with how many lines? Are these results pooled together from both lines? How many times did you repeat the differentiation process from hiPCS towards mature astrocytes?
We have added this information to the manuscript in lines 112-117 and 756-757. differentiation process from hiPSC to vmAstro was repeated 5 times. Again, we have data which we have not included in this manuscript but demonstrates that 3 independent differentiations from one of the NAS2 hiPSC line generated a population of vmAstros where 97.4% expressed S100β and 99.6% expressed FOXA2 (n=3, independent replicates sem 2.3 ; 0.4 respectively). In total the differentiation process from hiPSC to vmAstro has been repeated 6 times. In addition, the protocol to generate vmNPCs and subsequent ventral midbrain dopaminergic neurons has been carried out on multiple lines; 3 hiPSC lines (NAS2 and AST23, both from Dr Tilo Kunath, University of Edinburgh and MSU-H001, a gift from Prof. Jose Bernardo Cibelli, Michigan State University) and a hESC line (Shef6, UK Stem Cell Bank), all with comparable results (Stathakos, Jimenez-Moreno et al. 2019, Stathakos, Jimenez-Moreno et al. 2020).

Reviewer #2:
Manuscript Summary:
In the manuscript "Efficient and scalable generation of human midbrain astrocytes from hiPSCs" the authors demonstrate a protocol for specification and generation of ventral midbrain astrocytes (vmAstros) from hiPSCs and suggest that the resultant cells express astrocytic markers, as well as markers specific to the ventral midbrain. Additionally, the authors comment on the scalability of their protocol, and suggest that their methodology allows for an expansion of progenitors up to 4000 175cm2 flasks, allowing for cryopreservation of cells in the progenitor state for rapid use in experimentation. Furthermore, the authors demonstrate that their hiPSC derived vmAstros respond to the pro-inflammatory cytokines IL-1α and IL-1β and subsequently increase secretion of IL-6, thus suggesting that the derived astrocytes are 'reactive' in nature. Though the manuscript is well written and the protocol seems feasible, the main concerns of this reviewer relate to its relevance in a field with multiple well established protocols already present, and furthermore the true identity of the derived cells as being ventral midbrain in nature with little to no contamination by other regions.

Major Concerns:
Specific Comments:
1. Were other ventral midbrain markers, such as LMX1A, CORIN, EN1, in addition to FOXA2 been examined since this marker is present in the basal plate dorsolateral to the floor plate as well as the ventral diencephalon and rhombencephalon? Without checking forebrain, hindbrain, and dorsolateral expression there is no way to know that FOXA2 and MSI1 is specific to the midbrain.
LMX1A and LMX1B expression is demonstrated by immunocytochemistry in figures 2E and F. We have also included for this response letter unpublished data that we intend to publish in a separate manuscript which further characterises the vmAstro phenotype. We demonstrate expression of the midbrain marker gene Engrailed-1 (*EN1*) throughout the differentiation stages, and expression of *EN1* is maintained in the mature astrocytes (Figure R1). We also demonstrate expression of the *DRD2* gene, which encodes Dopamine Receptor D2, expressed in the adult rodent ventral midbrain and required for the function of ventral midbrain astrocytes in vivo (Figure R1)(Xin, Schuebel et al. 2019). Published transcriptomic analysis of in vivo ventral midbrain astrocytes in the adult mouse brain has demonstrated that the *ITPR1* gene is highly enriched this population, compared to astrocytes from the hippocampus or cortex(Xin, Schuebel et al. 2019). We have demonstrated expression of its human homologue in the mature vmAstros (Figure R1). We hope that this information satisfies the reviewers concerns.

2. Previous literature shows that FGF-8b is needed to maintain vmNPCs identity, otherwise the phenotype defaults to diencephalic patterning. Repeated passaging in N2B27 media with BDNF, GDNF, and AA from day 10 to day 30 or 45 is likely to expand a forebrain-specific cell type, which also express LMX1A/B. Can the authors please comment on whether they have checked for expression of forebrain-specific markers. How are vmNPCs quality controlled prior to induction with Astro differentiation media?
We acknowledge that FGF8 is used in numerous hiPSC differentiation protocols for the generation of ventral midbrain dopamine neurons to mimic FGF signalling required for patterning the embryonic midbrain. For these reasons we have also previously investigated whether addition of FGF8 influences generation of

ventral midbrain progenitors and dopamine neurons, finding that in terms of the generation of ventral midbrain dopamine neurons, the inclusion of FGF8 had no effect (Stathakos, Jimenez-Moreno et al. 2020). The early stages of our protocol are based closely on that published by Kriks et al., 2011, who also demonstrated that FGF8 did not have a significant effect on the induction of midbrain floor plate. In fact CHIR99021 used in combination with SHH had the greatest effect (Kriks, Shim et al. 2011). Indeed, based on the findings by Kriks et al., there have been multiple published examples of protocols that differentiate midbrain floor plate precursors towards ventral midbrain dopamine neurons. Furthermore, we have demonstrated that the vmNPCs generated in the currect protocol, and from which we derive the vmAstros, express LMX1A, LMX1B, and FOXA2 (Stathakos, Jimenez-Moreno et al. 2020), and we also show these transcription factors are also present in the vmAstros (fig 2 E-G of submitted manuscript). In addition, we have data demonstrating sustained expression of midbrain marker EN1 at every stage of our protocol and also in the mature vmAstros (Figure R1). These data are for the reviewers' attention only, as they are to be be published on a manuscript currently in preparation, which focuses on the characterization and neuroinflammatory response of hiPSC-derived vmAstros (see note above).
In terms of quality control of vmNPCs prior to the induction of astrocyte differentiation, we regularly use ICC on vmNPC cultures for ventral midbrain markers LMX1A, LMX1B and FOXA2. We also use the same vmNPCs to differentiate ventral midbrain dopaminergic neurons- all vmAstros generated in body of work were differentiated from vmNPC cultures with the ability to ventral midbrain dopaminergic neurons expressing TH, DAT, LMX1A, LMX1B and FOXA2.

3. Previous literature has shown that optimization of CHIR and SHH concentrations is cell line-specific. Have the authors optimized CHIR and SHH based on expression of forebrain (Foxg1, Nkx-2.1, Dbx1), hindbrain (Gbx2, Hoxa2), and dorsolateral (Sim1, Nkx-2.2, Nkx-6.1, Brn3a) markers? What was the rationale for the use of 0.8 μM CHIR and 200 ng/mL SHH in the differentiation of vmNPCs for these lines? Can the authors comment on the applicability of this protocol if there is line to line variability?

We addressed the effects of CHIR and SHH concentrations on the generation of ventral midbrain dopaminergic neurons in our previously published work (Stathakos, Jimenez-Moreno et al. 2020). We showed that a range of between 0.6 and 0.8 μM, in combination with a SHH concentration range between 200-300 ng/ml gave the greatest number of ventral midbrain dopaminergic neurons, and the greatest expression of ventral midbrain markers FOXA1, LMX1A and CORIN. In terms of hiPSC line variability, the initial induction of ventral midbrain identity was compared across 3 hiPSC lines (NAS2 and AST23, both from Dr Tilo Kunath, University of Edinburgh and MSU-H001, a gift from Prof. Jose Bernardo Cibelli, Michigan State University) and a hESC line (Shef6, UK Stem Cell Bank), all with comparable results (Stathakos, Jimenez-Moreno et al. 2019, Stathakos, Jimenez-Moreno et al. 2020). The protocol for the generation of vmAstros, as detailed in this manuscript has been carried out in two iPSC lines, NAS2 and AST23 with equally consistent results.

4. Previously established protocols demonstrating generation of not only midbrain astrocytes, but other regionally specified astrocytes utilize Ciliary Neurotrophic Factor (CNTF) in the final differentiation phase. Though we understand that both CNTF and LIF share common activation patterns with respect to downstream signaling, can the authors comment on why LIF was chosen in this protocol and whether CNTF would exert similar effects and resultant cell differentiation? Do the authors believe that LIF exerts a greater effect than CNTF in these cells?

Although we did not directly quantify the differences, when we first started to optimise this protocol, we did test expansion of vmAPCs in combinations of EGF, FGF2, LIF and CNTF. LIF and CNTF are both activators of the JAK/STAT pathway, which provides transcriptional modulation required for astroglial fate acquisition; FGF2 and EGF and mitogens that promote proliferation of neural progenitors. Therefore, we trialled combinations of these factors to generate a proliferating vmAPC population. Comparing EGF and FGF2, we found that FGF2 gave greatest heterogeneity in cell morphology and eventual astrocyte marker expression, probably because FGF2 promotes proliferation of a wide range of neural progenitors, whereas EGF has been shown to specifically support proliferation of astroglial type progenitors (Watts, McConkey et al. 2005). We found that in the absence of LIF, even in the presence of CNTF, proliferation of the vmAPCs slowed significantly over extended culture periods. As we required a scalable protocol, and because it is well documented that acquisition of astroglial fate *in vitro* requires an extended period of culture, we chose to use LIF in combination with EGF.
It has been demonstrated in both neural and other cell types, that LIF is a more potent mitogen than CNTF: LIF is a potent activator of expression of human telomerase reverse transcriptase gene and therefore confers telomere stability to cells, enabling them to proliferate for longer periods in culture (Ostenfeld, Caldwell et al. 2000, Wang, Wu et al. 2008). In terms of neural cell culture, the effect of LIF on long term proliferation is particularly seen in human cells, which express lower levels of telomerase than their rodent

counterparts, and this is further reduced with time in culture, leading to a slowing of proliferation. The application of LIF prevents this (Ostenfeld, Caldwell et al. 2000).
However, in this protocol LIF plays two roles in the generation of vmAstros- as described it enables long term expansion of vmAPCs. However, we also retain LIF in the maturation of vmAstros in combination with BMP4. In this context, with active BMP signalling, the transcriptional targets downstream of LIF are altered due to direct binding of BMP signal transducers to LIF induced transcriptional complexes. This modifies the transcriptional effects, including shifting neural cell fate towards acquisition of a mature astrocyte phenotype development (Nakashima, Yanagisawa et al. 1999, Nakashima, Yanagisawa et al. 1999).

5. The authors demonstrate their protocol extending to 90+ days (Figure 1) and show S100β staining of their resultant cells. Recent studies have demonstrated that S100β is a better marker of early stage immature astrocytes which establishes peak expression in a significant portion of cells by 90 days, whereas the widely accepted marker of mature astrocytes, GFAP, only starts to be expressed by 90 days, and requires a full 180 days in vitro to reach peak expression before a majority of cells exhibit GFAP staining. Can the authors demonstrate GFAP staining in their cells, which would suggest that they are indeed generating fully mature astrocytes?

Thank you for your suggestions. We have now added GFAP staining images to the manuscript (Figure 2H). In addition, we have included in this letter additional data that we will publish in a separate manuscript which shows that the mature astrocyte gene *ALDH1L1* is highly upregulated in vmAstros compared to vmAPCs suggesting the treatment with BMP4 and LIF is resulting in maturation (Figure R1).

6. With regard to the authors demonstration of reactivity in response to IL-1α and IL-1β, there is evidence that astrocyte reactivity does not exist in a finite state, similar to that seen in macrophages and microglia, rather there is a continuum of activation and these cells can exist in multiple reactive states reflected by different phenotypes. The treatment of cells with IL-1α would presumably result in a shift to what is considered an A1 phenotype, whereas IL-1β results in a more mixed expression of both A1 and A2 classifications. Can the authors comment on the activation phenotype they demonstrate, and also examine markers of reactivity for both A1 and A2 phenotypes to demonstrate which classification their cells fall into? An understanding of how these cells respond and react would be key in deepening our understanding of how presumptive vmAstros would respond in vivo.

In our upcoming manuscript we examine astrocyte reactivity in detail. Liddelow et al., 2017 was one of the first in depth studies to define the A1 and A2 subtype, and this group have furthered this work with numerous consecutive publications(Liddelow, Guttenplan et al. 2017). Recently they examined the A1/A2 subtype in hiPSC derived astrocytes (Barbar, Jain et al. 2020). What they demonstrate is that the A1 and A2 reactive phenotypes are defined by specific transcriptional changes in the astrocytes(Liddelow, Guttenplan et al. 2017). Some of these changes are unique either A1 or A2 in all scenarios, and some of these transcriptional changes fall in more of a context specific category(Liddelow, Guttenplan et al. 2017, Barbar, Jain et al. 2020). In addition, depending in the gene the variability in reproducibilty is rather large and there are species specific variations(Liddelow and Barres 2017, Barbar, Jain et al. 2020). However, by treating vmAstros with IL-1α, IL-1β, IL-6, TNF-α and combinations of these with other factors, such as complement factor C1q, we have been able to elucidate the shift towards reactivity in vmAstros. As the preliminary data in Figure R2 C demonstrates, by treating with IL-1α and IL-1β we generate upregulation of both Pan (*LCN2* & *ICAM1*) and A1 specific (*AMIGO2*) reactivity markers (Figure R2 C). We are currently extending this data to examine genes associated with the A1, A2 and pan reactivity transcriptome specifically in human astrocytes. We hope when complete this data will give us a better understanding of astrocyte reactivity in the midbrain and we are also examining how this then impacts neuronal health.

7. The ventral midbrain is complex and it is well established that each sub-region plays a role in distinct behaviors. Recent studies have demonstrated a significant difference in the transcriptional profile of midbrain astrocytes, as well as significant differences in their neuroprotective capabilities with regard to their neighboring ventral midbrain dopamine neurons. Given this heterogeneity, can the authors comment on which sub-region (ventral tegmental area or substantia nigra) they believe these iPSC derived vmAstros would be? Have the authors explored any mechanism by which a mixed population of vmAstros could be subsequently separated into sub-regional astrocyte populations for experimentation?

This is a great suggestion. We have considered this, particularly in light the publication by Xin et al., where the in vivo midbrain astrocyte phenotype is looked at in more detail. We have not yet formally determined whether our vmAstros are more similar to VTA or Substantia nigra (SN). We can confirm expression of *ITPR1* (Figure R1), identified by Xin et al., 2019 as enriched in ventral midbrain astrocytes, but as the authors did not differentiate between VTA or SN (Xin, Schuebel et al. 2019), its usefulness as a regional

stratification marker is unclear. Kostuk et al., 2019 carried out a direct transcriptomic and secretomic analysis on VTA versus SN mouse astrocytes, and when viewing their data, we can see that ITPR1 is expressed at relatively similar levels in VTA and SN astrocytes (Kostuk, Cai et al. 2019). Therefore, at this point in our examination of the vmAstros, we are unable to provide clear evidence of a definitive VTA or SN subtype- however we are currently carrying out some high-content analysis of the proteins expressed by the vmAstros and we hope this will provide further elucidation.

Minor Concerns:
8. Figure 2B shows expression of the pan neuronal marker TUJ1 in the red channel, however the figure legend identifies the red channel as TH. Additionally, panel 3 of row G lacks a label denoting what the stain is. Please clarify
Thank you for highlighting this- we have corrected the figure.

Reviewer #3:
Manuscript Summary:
This is a well written protocol which is easy to follow and seems to contain all relevant information required including stock concentrations, images of the differentiating cells at different stages of the protocol and characterisation of the resultant cells. The figures are clear, well described and pertinent to the text. I have no concerns or edits to request.
Thank you for your positive comments.

Reviewer #4:
Manuscript Summary:
The authors have developed a new protocol to generate ventral midbrain astrocytes (vmAstros) from hiPSCs. Although the paper is very well explained with several details included, I have some suggestions that might improve the outcome.

Major Concerns:
1. The authors point only 10 days for astrocyte's maturation. Isn't it too short? The authors should demonstrate their maturity not only by GLAST and S100b expression, but use other markers of mature astrocytes, such as GFAP, AQP4, Vimentin and perhaps the newly identified CD49f marker. Moreover, some gene expression analysis should be included to compare immature astrocytes with mature ones. I would suggest to include foetal immature human astrocytes as control and analyse whether the generated astrocytes express immature astrocytes markers such as NUSAP1 and CD44. Additionally, the authors could check whether hiPSC derived astrocytes express the human-specific astrocyte markers identified by Zhang et al. 2016 such as LRRC3B, STOX1, RYR3, MRVI1 and FAM198B.
We have included data in this rebuttal letter to satisfy the reviewer, but we do not wish to include this in the JOVE manuscript (see Figure R1, above). We show that exposure to BMP4 in combination with LIF in the maturation stage of the protocol leads to large increase in expression of *ALDH1L1,* which in Zhang et al. 2016 is used to identify the mature astrocytes. In Figure R1 we also demonstrate that the mature vmAstros demonstrate increased expression of the *DRD2,* compared to vmAPCs. Homologues of *DRD2* are crucial to the function of ventral midbrain astrocytes in the adult rodent brain (Cahoy, Emery et al. 2008, Xin, Schuebel et al. 2019) (Figure R1). Similarly, we demonstrate expression of *ITPR1*, the homologue of which is highly enriched in adult rodent ventral midbrain astrocytes, compared to those of the hippocampus or cortex (Xin, Schuebel et al. 2019) (Figure R1). In addition, as suggested by the reviewer, we have now included images in figure 2 to demonstrate specific expression of GFAP and the mature astrocyte marker CD49f, which is also enriched with maturation (Figure 2I)(Barbar, Jain et al. 2020, Barbar, Rusielewicz et al. 2020). The experiment suggested by the reviewer to compare the expression of these genes and proteins between hiPSC-derived vmAstros and those from human fetal tissue would be valuable, but unfortunately we are unable to access human fetal tissue to carry out these experiments and we hope the reviewer will accept that due to the requirements for handling such tissue this is not something we are able to complete.

2. The authors should assess astrocyte functionality by evaluating calcium activity, phagocytosis or glutamate uptake. It would be interesting to assess whether iPSC-derived astrocytes have the capacity to support neuronal function by co-culturing those astrocytes with iPSC-derived neurons and measuring neuronal-action potentials by electrophysiological recordings, or neurite length.
We are currently carrying out calcium imaging and looking at responses to glutamate within this for our next publication. We can state that the hiPSC-vmAstros demonstrate intrinsic calcium signalling and respond to particular stimulation. As shown in Figure R2 the vmAstros are able to phagocytose α-synuclein and neuronal debris- this data will form part of our next manuscript detailing further characterisation of the vmAstro phenotype in relation to neuroinflammation. In addition, we are currently carrying out co-culture

experiments to examine how the vmAstros influence the function and survival of dopaminergic neurons, again this data will be included in our other manuscript.

3. The authors should show a quantification of the astrocyte purity in the culture by showing the percentage of positive expression of neuronal markers.
As stated in response to previous comments 97.4% expressed S100β and 99.6% expressed FOXA2 (n=3, independent replicates sem 2.3 ; 0.4 respectively)

Minor Concerns:
1. How many passages could be done in mature astrocytes?
No passages as such because as stated in the manuscript the proliferation rate should be very low, but they can be replated for specific assays at a desired density. We usually do this after the 10 day maturation period. We have modified the manuscript to make this clear (line 489 onwards).

2. For how long hiPSC-derived astrocytes could be maintained in culture for a specific experiment? Do they get reactive while they are in culture?
After the 10-day maturation period we replace the media with Astro media without BMP4 and LIF and maintain them in this for 72 hours prior to carrying our experiments. This was omitted from the original submission- we have now included these details (line 489 onwards). This is because we have some data that the presence of BMP4 and LIF, or the residual signalling can interfere with neuroinflammatory stimulation. We have extended this post-maturation period to up to 7 days without any obvious effect. However, we do think that components of the Geltrex ECM degrade or are washed off over time as we see vmAstros (or vmAPCs) begin to shrink and eventually lift off the culture surface after upwards of 14 days. Therefore, we would advise replating after 10 days of either vmAPCs or vmAstros.
In terms of reactivity we do not see that the vmAstros have become reactive unless specifically stimulated (Figure 2J-L and Figure R2). However, without looking at reactivity markers in individual vmAstros we cannot rule out that a small subpopulation are reactive in basal conditions.

3. What is the percentage of confluent cells when starting the differentiation of vmNPC?
When we begin the induction of vmNPCs, the hiPSCs are approximately $4–5x10^4$ cells/cm^2, as shown in Figure 1 (Stathakos, Jimenez-Moreno et al. 2020). We have added this detail to the protocol (line 331 onwards).
For how long can you split vmNPCs? The vmNPCs are expanded up to day 50 of the protocol, splitting approximately every 3-4 days (line 447 onwards).

Do they mature while splitting them?
Yes, we have previously shown that post day 30 the vmNPC population begins to express more mature neuronal markers (Stathakos, Jimenez-Moreno et al. 2020), indicating a subpopulation of mature/maturing neurons within the vmNPC culture. However, use of vmNPC cultures up to day 50 to generate vmAPCs has shown no effect on the astrocyte differentiation potential. We assume that this is because any terminally differentiated neurons are unable to survive the high ratio passaging employed in the expansion of vmAPCs.

4. Section 3.3. The authors mentioned the use vmNPCs cultures "as in stage 1". What does it mean? Are they cultured in induction or maintenance media (N2B27 + GDNF + BDNF + ascorbic acid)? Clarify this point.
We have attempted to clarify this point by rewording (line 447 onwards).

5. Section 3.3.9. What are the characteristics of these cells? Which markers do they express? Are they highly proliferative cells? Why the authors decided to expand them until day 90?
The vmAPCs remain highly proliferative until at least day 120. We used day 90 expanded cultures because previous studies generating astrocytes from hiPSC or hESCs have shown this as an appropriate time frame for neural progenitors to efficiently generate astrocytes. However, we acknowledge this varies depending on methodology and cell lines used (Crompton, Cordero-Llana et al. 2017).
In Figure R1 we demonstrate expression of various genes throughout the different stages of the protocol. For example, the midbrain marker EN1 and the astrocyte marker ALDH1L1. ALDH1L1 expression increases significantly upon maturation (Figure R1)

Barbar, L., T. Jain, M. Zimmer, I. Kruglikov, J. S. Sadick, M. Wang, K. Kalpana, I. V. L. Rose, S. R. Burstein, T. Rusielewicz, M. Nijsure, K. A. Guttenplan, A. di Domenico, G. Croft, B. Zhang, H.

Nobuta, J. M. Hebert, S. A. Liddelow and V. Fossati (2020). "CD49f Is a Novel Marker of Functional and Reactive Human iPSC-Derived Astrocytes." Neuron **107**(3): 436-453 e412.
Barbar, L., T. Rusielewicz, M. Zimmer, K. Kalpana and V. Fossati (2020). "Isolation of Human CD49f(+) Astrocytes and In Vitro iPSC-Based Neurotoxicity Assays." STAR Protoc **1**(3): 100172.
Cahoy, J. D., B. Emery, A. Kaushal, L. C. Foo, J. L. Zamanian, K. S. Christopherson, Y. Xing, J. L. Lubischer, P. A. Krieg, S. A. Krupenko, W. J. Thompson and B. A. Barres (2008). "A Transcriptome Database for Astrocytes, Neurons, and Oligodendrocytes: A New Resource for Understanding Brain Development and Function." Journal of Neuroscience **28**(1): 264-278.
Cortes, D., O. A. Carballo-Molina, M. J. Castellanos-Montiel and I. Velasco (2017). "The Non-Survival Effects of Glial Cell Line-Derived Neurotrophic Factor on Neural Cells." Front Mol Neurosci **10**: 258.
Crompton, L. A., O. Cordero-Llana and M. A. Caldwell (2017). "Astrocytes in a dish: Using pluripotent stem cells to model neurodegenerative and neurodevelopmental disorders." Brain Pathol **27**(4): 530-544.
Kostuk, E. W., J. Cai and L. Iacovitti (2019). "Subregional differences in astrocytes underlie selective neurodegeneration or protection in Parkinson's disease models in culture." Glia **67**(8): 1542-1557.
Kriks, S., J.-W. Shim, J. Piao, Y. M. Ganat, D. R. Wakeman, Z. Xie, L. Carrillo-Reid, G. Auyeung, C. Antonacci, A. Buch, L. Yang, M. F. Beal, D. J. Surmeier, J. H. Kordower, V. Tabar and L. Studer (2011). "Dopamine neurons derived from human ES cells efficiently engraft in animal models of Parkinson's disease." Nature **23**(7378): 215-551.
Liddelow, S. A. and B. A. Barres (2017). "Reactive Astrocytes: Production, Function, and Therapeutic Potential." Immunity **46**(6): 957-967.
Liddelow, S. A., K. A. Guttenplan, L. E. Clarke, F. C. Bennett, C. J. Bohlen, L. Schirmer, M. L. Bennett, A. E. Munch, W. S. Chung, T. C. Peterson, D. K. Wilton, A. Frouin, B. A. Napier, N. Panicker, M. Kumar, M. S. Buckwalter, D. H. Rowitch, V. L. Dawson, T. M. Dawson, B. Stevens and B. A. Barres (2017). "Neurotoxic reactive astrocytes are induced by activated microglia." Nature **541**(7638): 481-487.
Nakashima, K., M. Yanagisawa and H. Arakawa (1999). "Synergistic Signaling in Fetal Brain by STAT3-Smad1 Complex Bridged by p300 | Science."
Nakashima, K., M. Yanagisawa, H. Arakawa and T. Taga (1999). "Astrocyte differentiation mediated by LIF in cooperation with BMP2." FEBS Lett **457**(1): 43-46.
Ostenfeld, T., M. A. Caldwell, K. R. Prowse, M. H. Linskens, E. Jauniaux and C. N. Svendsen (2000). "Human neural precursor cells express low levels of telomerase in vitro and show diminishing cell proliferation with extensive axonal outgrowth following transplantation." Exp Neurol **164**(1): 215-226.
Stathakos, P., N. Jimenez-Moreno, L. Crompton, P. Nistor, M. A. Caldwell and J. D. Lane (2019). "Imaging Autophagy in hiPSC-Derived Midbrain Dopaminergic Neuronal Cultures for Parkinson's Disease Research." Methods Mol Biol **1880**: 257-280.
Stathakos, P., N. Jimenez-Moreno, L. A. Crompton, P. A. Nistor, J. L. Badger, P. A. Barbuti, T. L. Kerrigan, A. D. Randall, M. A. Caldwell and J. D. Lane (2020). "A monolayer hiPSC culture system for autophagy/mitophagy studies in human dopaminergic neurons." Autophagy: 1-17.

Wang, X., H. Wu, Z. Zhang, S. Liu, J. Yang, X. Chen, M. Fan and X. Wang (2008). "Effects of interleukin-6, leukemia inhibitory factor, and ciliary neurotrophic factor on the proliferation and differentiation of adult human myoblasts." Cell Mol Neurobiol **28**(1): 113-124.
Watts, C., H. McConkey, L. Anderson and M. Caldwell (2005). "Anatomical perspectives on adult neural stem cells." J Anat **207**(3): 197-208.
Xin, W., K. E. Schuebel, K. W. Jair, R. Cimbro, L. M. De Biase, D. Goldman and A. Bonci (2019). "Ventral midbrain astrocytes display unique physiological features and sensitivity to dopamine D2 receptor signaling." Neuropsychopharmacology **44**(2): 344-355.
Yun, S. P., T. I. Kam, N. Panicker, S. Kim, Y. Oh, J. S. Park, S. H. Kwon, Y. J. Park, S. S. Karuppagounder, H. Park, S. Kim, N. Oh, N. A. Kim, S. Lee, S. Brahmachari, X. Mao, J. H. Lee, M. Kumar, D. An, S. U. Kang, Y. Lee, K. C. Lee, D. H. Na, D. Kim, S. H. Lee, V. V. Roschke, S. A. Liddelow, Z. Mari, B. A. Barres, V. L. Dawson, S. Lee, T. M. Dawson and H. S. Ko (2018). "Block of A1 astrocyte conversion by microglia is neuroprotective in models of Parkinson's disease." Nat Med **24**(7): 931-938.